

UNCLASSIFIED

AD NUMBER
AD906561
NEW LIMITATION CHANGE
TO Approved for public release, distribution unlimited
FROM Distribution authorized to U.S. Gov't. agencies only; Test and Evaluation; SEP 1977. Other requests shall be referred to Air Force Cambridge Research Laboratories, Attn: LQP, L. G. Hanscom Field, Bedford, MA 01730.
AUTHORITY
AFCRL ltr, 21 Aug 1974

THIS PAGE IS UNCLASSIFIED

✓
AFCRL 72-0452

AD906561

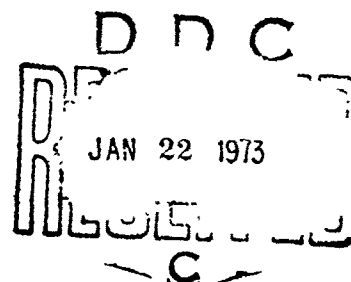
EVALUATION OF LASER WINDOW MATERIALS

by

Larry L. Hench, Derek B. Dove and Ronald E. Loehman

Engineering and Industrial
Experiment Station
University of Florida
Gainesville, Florida 32601

Contract No. F19628-71-C-0256
Project No. 3326
Task No. 332605
Work Unit No. 33260501



FINAL REPORT

Period Covered: July 1, 1971 Through June 30, 1972

August 1, 1972

Contract Monitor: Alton F. Armington
Solid State Sciences Laboratory

Distribution limited to U.S. Government agencies only;
Test and Evaluation, 19 September 1972. Other request
for this document must be referred to AFCRL (LQP), L.G.
Hanscom Field, Bedford, Massachusetts 01730.

Prepared for

AIR FORCE CAMBRIDGE RESEARCH LABORATORIES
AIR FORCE SYSTEMS COMMAND
UNITED STATES AIR FORCE
BEDFORD, MASSACHUSETTS 01730

**Best
Available
Copy**

Qualified requestors may obtain additional copies
from the Defense Documentation Center.

EVALUATION OF LASER WINDOW MATERIALS

by

Larry L. Hensch, Derek B. Dove and Ronald E. Loehman

Engineering and Industrial
Experiment Station
University of Florida
Gainesville, Florida 32601

Contract No. F19628-71-C-0256
Project No. 3326
Task No. 332605
Work Unit No. 33260501

FINAL REPORT

Period Covered: July 1, 1971 Through June 30, 1972

August 1, 1972

Contract Monitor: Alton F. Armington
Solid State Sciences Laboratory

Distribution limited to U.S. Government agencies only;
Test and Evaluation, 19 September 1972. Other request
for this document must be referred to AFCRL (LQP), L.G.
Hanscom Field, Bedford, Massachusetts 01730.

Prepared for

AIR FORCE CAMBRIDGE RESEARCH LABORATORIES
AIR FORCE SYSTEMS COMMAND
UNITED STATES AIR FORCE
BEDFORD, MASSACHUSETTS 01730

Abstract

In an attempt to evaluate the limitations of glasses as high power laser windows, chalcogenide glasses of several compositions within the Ge-Se-As system have been prepared and characterized before and after heat treatment. The glasses are homogeneous to a fine scale, but appreciable optical absorption at $10.6\mu\text{m}$ is present, due to the presence of oxygen impurities. The effect of gettering additions of Ti and Zr in the glasses to decrease the infrared absorption has been examined with limited success. Fabrication in purified graphite crucibles as a means of decreasing impurity absorption has been investigated. Heat treatment shows that the glasses prepared in our laboratory as well as commercial Texas Instruments glasses are stable against devitrification and may withstand many hours of thermal exposure at 300°C without significant change in mechanical properties.

A novel attempt to increase the toughness and water resistance of sintered alkali halide windows has been carried out by coating the alkali halide grains with polyethylene prior to hot pressing. The two materials were chosen since they have a reasonably good refractive index match. Results, however, have been disappointing owing to the difficulty of obtaining a really coherent coating. The approach warrants further effort but requires a more detailed study of the chemistry of the inorganic-organic interface than could be carried out under the present program. The results of limited tests of the increase in water resistance imparted by coatings of deposited chalcogenide glasses are reported.

Table of Contents

	<u>Page #</u>
Abstract	
I Introduction and Objectives	1
II Potentiality for Low IR Absorption in Chalcogenide Glasses at 10.6 μ m	2
III Choice of Glass System	4
IV Preparation of Chalcogenide Glasses	5
V Structural Studies of Chalcogenide Glasses	7
VI Infrared Behavior of Glassy Selenium	16
VII Infrared Behavior of Chalcogenide Glasses	16
VIII Thermal Treatment Studies of Chalcogenide Glasses	23
A. X-Ray Analysis	23
B. Crystallization Studies	23
C. Density Variations	29
D. Mechanical Property Studies	29
IX Coated Polycrystalline Alkali Halides	33
A. Nature of The Problem	33
B. Polymer Coatings	35
C. Chalcogenide Coatings	43
X Conclusions	45
XI References	47
XII Appendix A	49
XIII Appendix B	62

I. Introduction

The general objective of this research project was to determine means for enhancing the utility of glasses and alkali halides as high power laser windows. Analysis of the limitations of glasses as high power laser windows indicates that either structural heterogeneities or compositional impurities may increase IR absorption at 10.6 microns to an unsuitable level. Mechanical strength and thermal stability of candidate chalcogenide glasses also pose possible limitations on the suitability of these materials for laser windows. Consequently, specific experimental objectives for the study of high power laser window glasses were defined as:

- 1) Determine the limits of homogeneity for chalcogenide glasses containing Ge-Se-Sb-As-Te using both thin film and bulk fabrication techniques.
- 2) Evaluate the thermal stability of thin film and bulk chalcogenide glasses with good IR transmission.
- 3) Determine the impurity source of high IR absorption at 10.6 μ m in Ge-Se-As based glasses.
- 4) Decrease the impurity contribution in chalcogenide glasses by internal gettering, compositional adjustment, and thermal treatment.
- 5) Measure the mechanical properties of IR transmitting chalcogenide glasses and determine the effect of thermal history on the properties.

Evaluation of the limitations of alkali halides for high power laser windows indicates two major areas of deficiency: (1) poor mechanical strength, and (2) poor corrosion resistance. Our decision was to tackle both problems simultaneously by investigating the fabrication of polycrystalline alkali halide compacts using coated alkali halide granules. Specific research objectives were:

- 1) Select an organic coating-alkali halide system that satisfies complex IR window materials requirements.
- 2) Develop granule coating process.
- 3) Fabricate coated granules into test windows.
- 4) Develop chalcogenide glass coated granules, fabricate windows, and test properties and corrosion resistance.

The results achieved in the exploratory glass and alkali halide window research programs are presented in the following sections of this report.

II. Potentiality for Low IR Absorption in Chalcogenide Glasses at 10.6 μ m

Glasses possess several extremely valuable characteristics that make them important materials for the fabrication of optical components:

- 1) ease of component fabrication by casting, grinding and polishing.
- 2) properties may be varied continuously (within certain limits) by varying composition.

The extremely low absorption coefficient requirement for the 10.6 μ m window has, however, only been achieved so far in certain crystalline materials [1] and it is necessary to assess the possibility of obtaining glasses with sufficiently low absorption coefficients.

The transmission of radiation through a medium, glass or otherwise, may be affected by two major processes, absorption and scattering. Table I indicates some processes for consideration and their relevance to materials selection.

Several considerations emerge for the choice of glass for a 10.6 μ m window.

- 1) Optical heterogeneities should be absent or minimized by keeping fluctuations in the refractive index small and the scale of heterogeneities small compared with 10.6 μ m.
- 2) Impurities (particularly oxygen) should be controlled to lower than parts per million in the finished glass.
- 3) The following question should be answered, "Is there a fundamental absorption process intrinsic to the glassy condition that may prevent the achievement of an absorption coefficient as low as that achieved by the best crystalline materials?"
- 4) If the preceding considerations can be satisfactorily accounted for, then window design could in principle proceed by optimizing window figure of merit through variation in composition. Ease of fabrication, compatibility with optical coatings and resistance to environmental corrosion are questions that may be faced at a later date in the design process.

It is instructive to examine the properties of glasses in the visible range. Much interest is being generated by the possible use of glass fibers as transmission lines for the

Table I

Process	Comments
<u>Absorption</u>	
Atomic Vibrational	
a) Fundamental and Harmonic atomic Vibrations	Choose material with fundamental band far removed from $10.6\mu\text{m}$; Covalent bonding preferred to ionic bonding.
b) Impurities	Crystal growth techniques may aid in obtaining very high purity; severe problem in maintaining levels lower than ppm in glasses.
Electronic Processes	
a) Free carrier absorption	Minimize by choosing material of very high resistivity and limiting operational temperature excursions.
b) Localized states within energy gap	The presence of an appreciable density of localized states within the energy gap could give rise to absorption contributions at infrared wavelengths. This is normally referred to as absorption edge tailing although this has also been observed in some crystalline materials.

<u>Light Scattering</u>	Essentially due to local fluctuations in refractive index due to grain boundaries, presence of several phases, compositional fluctuations, density fluctuations, and ultimately thermal fluctuations. Extremely dependent on scale of optical inhomogeneity. Usually controlled in a glass by choice of composition and control of preparative technique. May or may not be accentuated at elevated temperatures.

transmission of information over distances of order miles. Evidently, extremely high transmission of radiation is required and some effort has been expended to examine the merits of various glasses for this application. In a review talk, D.J. Thomas [2] of Bell telephone laboratories reported that absorption values of 1.2×10^{-3} , 7.3×10^{-4} and $2 \times 10^{-4} \text{ cm}^{-1}$ had been measured at Bell Telephone Laboratories for Schott F2 glass, fused quartz and crystalline quartz respectively in the visible range. Light scattering was very low and measurements along the length of fibers revealed that some regions existed with extremely low losses.

Experience with glasses in the visible region has indicated that improvements in purity and homogeneity lead to better optical transmission. Although the excitation processes involved in the infrared glasses are different from those in the visible, essentially the same considerations apply concerning purity and homogeneity. The basic question concerning the existence of an inherent limit to optical transmission due to phenomena arising from the glassy structure appears to be unanswered at this time. Present theories imply the existence of a distribution of localized electronic states within the energy gap and hence optical absorption due to electronic excitation from these states into the conduction band is a possibility that requires further investigation.

Therefore, there does not appear at this time any firm scientific basis for ascribing a fundamental absorption process to amorphous structures, per se; consequently, it is justified to evaluate the contributions of structural heterogeneities and impurities on IR absorption. If these contributions can be eliminated from glasses there appears to be reasonable expectation that a suitable window material will result.

III. Choice of Glass System

Glasses comprised of Ge-Se-As-Sb-Te elements were evaluated in the program because of previous studies showing high IR transmission for these materials [3]. In particular, the Ge-Se-As system was chosen for much of the present work since it is known to possess a wide composition range within which glasses can be formed. The glass does not appear to phase separate, is known to be highly transparent in the infrared [3], and is resistant to devitrification.

In addition, a $\text{Ge}_{13}\text{Se}_{55}\text{As}_{12}$ Glass (TI-20) is available commercially to compare with experimental compositions. Compositions chosen for study are primarily $\text{GeSe}_2 + x\text{As}_2\text{Se}_3$. GeSe_2 in glassy form is the structural analogue of SiO_2 , the important glass former for glasses in the visible region. (It is not known, however, whether the Ge and Se atoms compositionally are as regularly ordered as are Si and O in SiO_2 .) The chosen compositional path connects two high temperature

end points across the ternary phase diagram. Unfortunately, the ternary diagram does not appear to be known. Figure 1 shows the glass forming region in this system as reported by Hilton and collaborators [4].

A further important consideration is that radial distribution studies on Ge-Te, Ge-Se and related glasses have indicated that the bonding in these materials is primarily covalent, a situation favorable for high infrared transmission [5], [6].

IV. Preparation of Chalcogenide Glasses

High purity Ge and As powder and Se shot were weighed into Vycor and quartz tubes. Each tube was sealed off under vacuum ($\sim 10^{-5}$ Torr) and heated in a resistance furnace at 900°C for at least five hours. In order to ensure homogeneity of the reacting material, the tubes were periodically shaken while in the furnace. The tubes were slowly cooled in the furnace for 3-1/2 hours to approximately 300°C , and were then removed from the furnace and allowed to cool to room temperature. It was found that too slow a quench resulted in the crystallization of the sample, whereas quenching too quickly caused the sample to crack into pieces, making infrared measurements difficult. All of the samples were found to adhere to the tube walls during the quench.

Disc-shaped samples of thickness 2.5mm and diameter 17 mm were cut from each tube using a diamond saw. The samples were ground with 600 grit SiC paper and polished with Al_2O_3 powder from 1 μm down to 0.05 μm .

Each polished sample was examined for the presence of internal defects such as crystallites and microvoids using an optical microscope equipped with an infrared image converter tube. Samples were subjected to x-ray diffraction analysis, optical microscopy and scanning electron microscopy. It was found that by using the correct quenching procedures the occurrence of crystallites and microvoids could be avoided. Thin films of selected compositions were obtained by flash evaporation of the bulk glasses onto glass, alkali halide, or mica substrates. Thicknesses in the range of 350 \AA -1000 \AA were achieved.

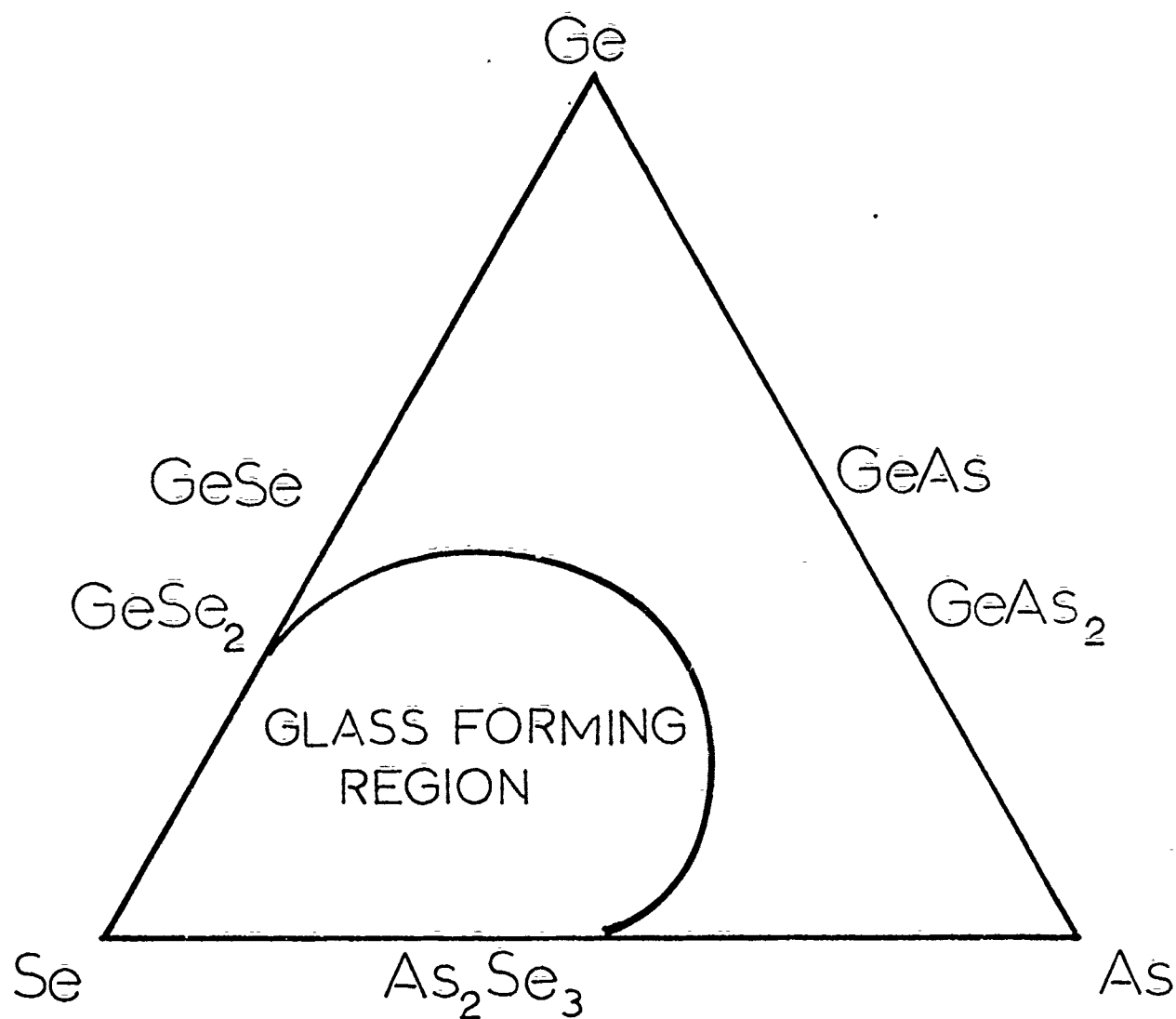


Fig. 1. Glass forming region in Ge-Se-As system [4].

V. Structural Studies of Chalcogenide Glasses

The properties of thin chalcogenide glass films have been the subject of study as part of a program [8] aimed at the characterization of the electrical and structural properties of amorphous semiconductors. Deposition from the vapor (by flash evaporation or sputtering, for example) provides a convenient method for the preparation of glass films over a wide range of compositions. Using thin film techniques, glasses have been prepared in film form that have not been attainable in bulk even with extreme quench rates.

Thin film glasses are of interest for a variety of electronic and dielectric applications and may be of significance for the laser window program as low absorption coatings for environmental protection and for optical impedance match. The films are in a form convenient for electron microscopy and diffraction.

As a preliminary to understanding optical and thermal properties of the glasses, it is necessary to characterize the structure on both an atomic level and on a macroscopic level. The type of bonding in the solid is of importance in determining the infrared response, while structural heterogeneity may give rise to undesirable light scattering.

The electron or x-ray diffraction pattern from a glass contains no sharp peaks owing to the lack of spatial periodicity in atomic positions. The pattern consists instead of diffuse halos or rings as from a gas or liquid. A statistical characterization of the local order may be obtained by carrying out a numerical Fourier transform of a particular function of the scattered intensity. This is a technique well understood in theory [9], but difficult to carry out reliably in practice owing to the presence of Compton background in the x-ray diffraction pattern or inelastically scattered electrons in the electron diffraction case.

The equipment employed in this laboratory has been developed to experimentally remove the Compton background in the x-ray case and to remove inelastically scattered electrons in the electron diffraction experiments. The Fourier transform yields a spectrum of interatomic distances with the glass; this spectrum is described as the radial distribution function (rdf). The position of peaks in the rdf provides a measure of interatomic distances, while areas under peaks are equal to mean coordination number times a function of the atomic scattering factor that frequently does not differ too widely from unity. The presence of several types of atoms in the glass complicates the interpretation of the rdf since a peak in the rdf may actually consist of a number of unresolved overlapping peaks. The interpretation of the rdf in terms of structural models then requires considerable care.

The results of the present authors [5] and others [6] working on the chalcogenides have shown that the interatomic distances within the glasses are consistent with primarily covalent bonding and coordination numbers are consistent with each atom retaining its "normal" valency, i.e., 4, 3, and 2 for Ge, As and Se or Te respectively. This is to be contrasted with the atomic structure of, for example, GeTe, GeSe₂ and others where interatomic distances are expanding and coordination is much higher than in the glass. Real differences in properties are therefore to be expected between these crystalline compounds and glasses of the same composition.

Figure 2 shows a drawing of the electron diffraction system [10] for measurements on thin films. The 50 kev electron beam is scattered on passing through the thin film, thus forming an electron diffraction pattern. A pair of coils immediately beneath the specimen magnetically deflects the electron diffraction pattern to and fro across a small aperture situated above an electrostatic filter and electron detector. The filter rejects inelastically scattered electrons (an important feature) and the transmitted electrons are measured as a function of scattering angle. Figure 3 shows a typical intensity versus scattering angle plot for a film of GeTe. Curve a is from the as-prepared film; curves b and c after heat treatment. Figure 4 shows the calculated radial distribution functions; the change in local order between curves a and c can be noted. The order change in this case corresponds to an increase in coordination number and probably is a precursor to the formation of crystallites. With further heating, crystallites form in the glass and sharp peaks begin to appear in the intensity curves.

X-ray diffraction studies were performed to compare thin film and bulk structures. Dr. R. W. Gould of the University of Florida has obtained x-ray intensity curves for several infrared glasses, as shown in Figures 5, 6 and 7 for the compositions Ge₂₈Se₁₂Sb₆₀ and Ge₃₃Se₅₅As₁₂ (obtained from Texas Instruments) and for Ge₃₃Se₅₅As₁₂ (University of Florida). Some differences in the last two curves may be seen, indicating possible differences in the degree of local ordering of glasses of the same composition prepared in different laboratories.

Electron microscopy has shown the glassy films to be homogeneous at least to a scale of order 20 Å. Figure 8 shows a film of GeTe₂ before and after heating in the electron microscope. Prior to heating (a) the film is essentially featureless and the diffraction pattern (b) is typical of a glass. After heating (c), crystallites can be clearly seen and the diffraction pattern (b) now contains sharp rings. In contrast, Roy and collaborators [11] have reported phase separation in bulk glasses containing tellurium. Therefore there appear to be appreciably fewer structured heterogeneities in the Te based glasses prepared as thin films than in

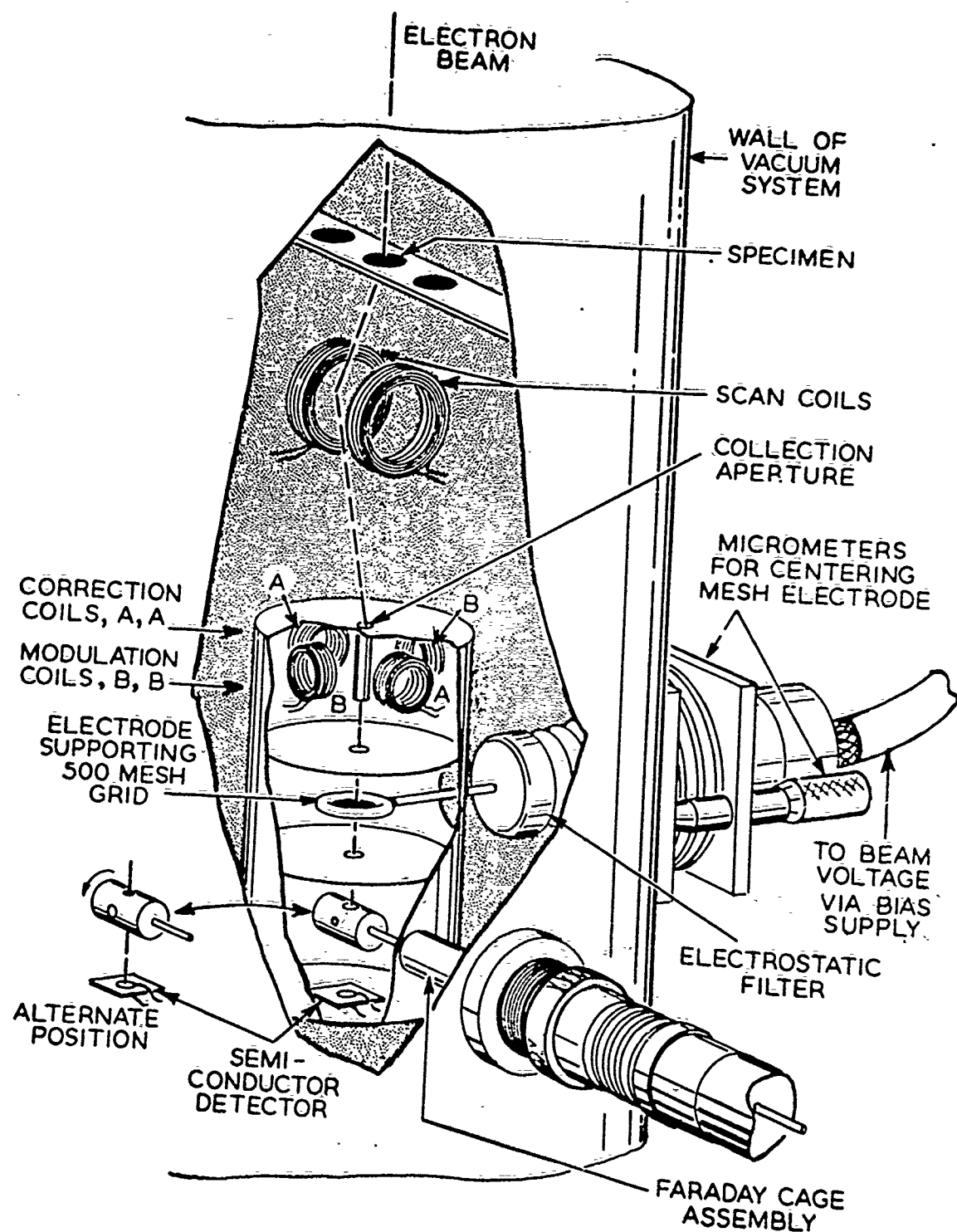


Fig. 2. Electron diffraction system.

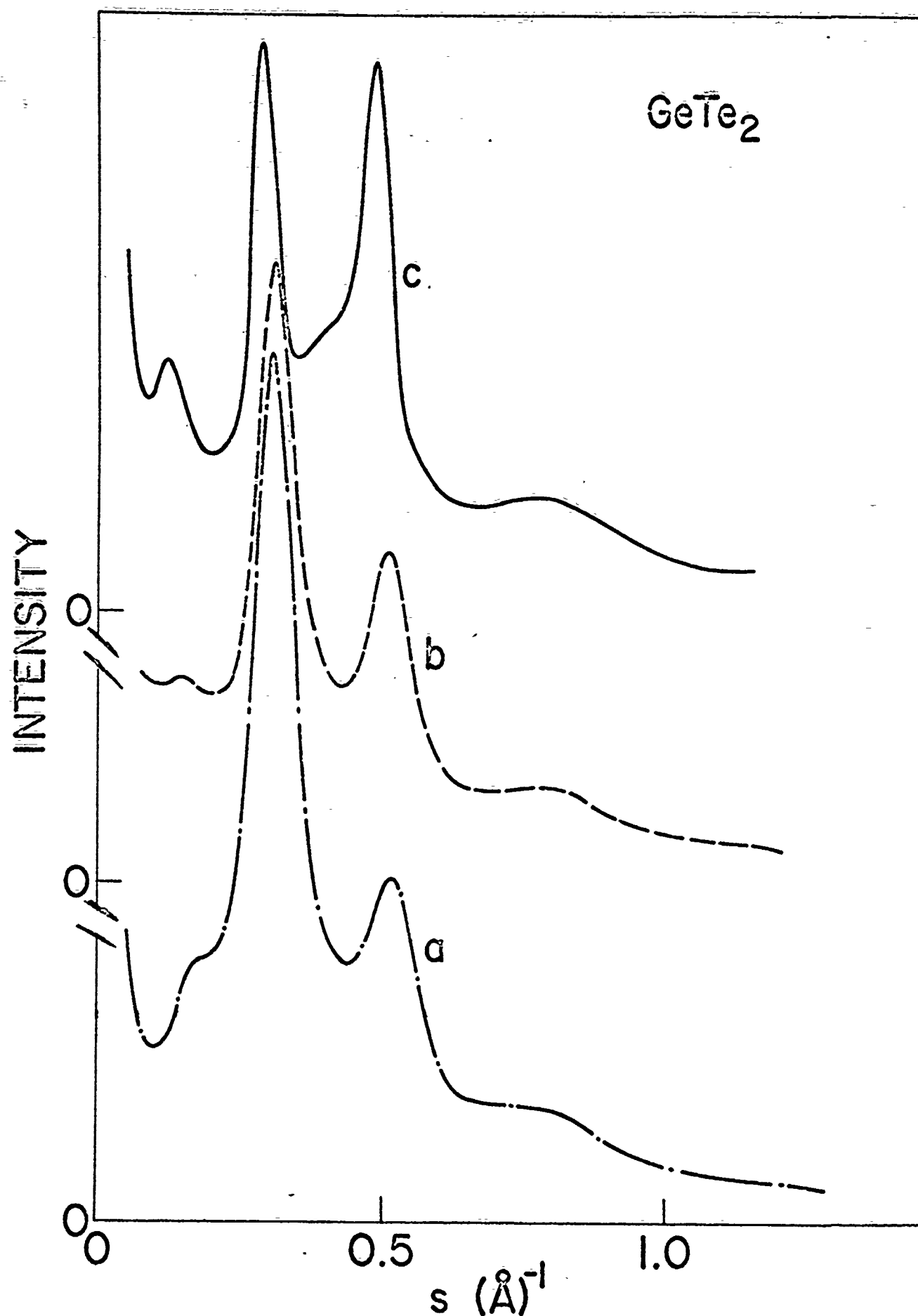


Fig. 3. Intensity as a function of scattering angle for GeTe_2 .

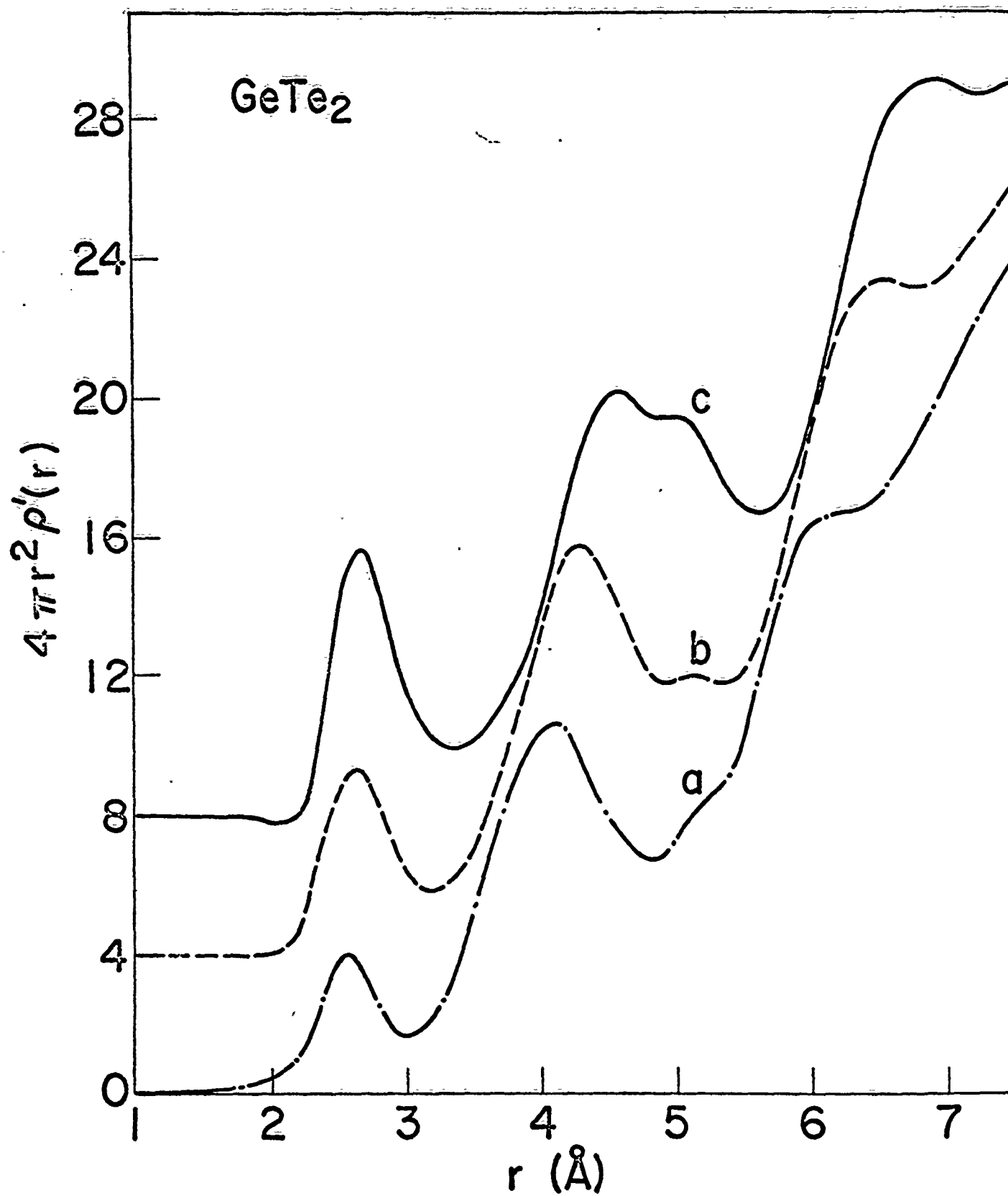


Fig. 4. Radial distribution function calculated from Fig. 3.

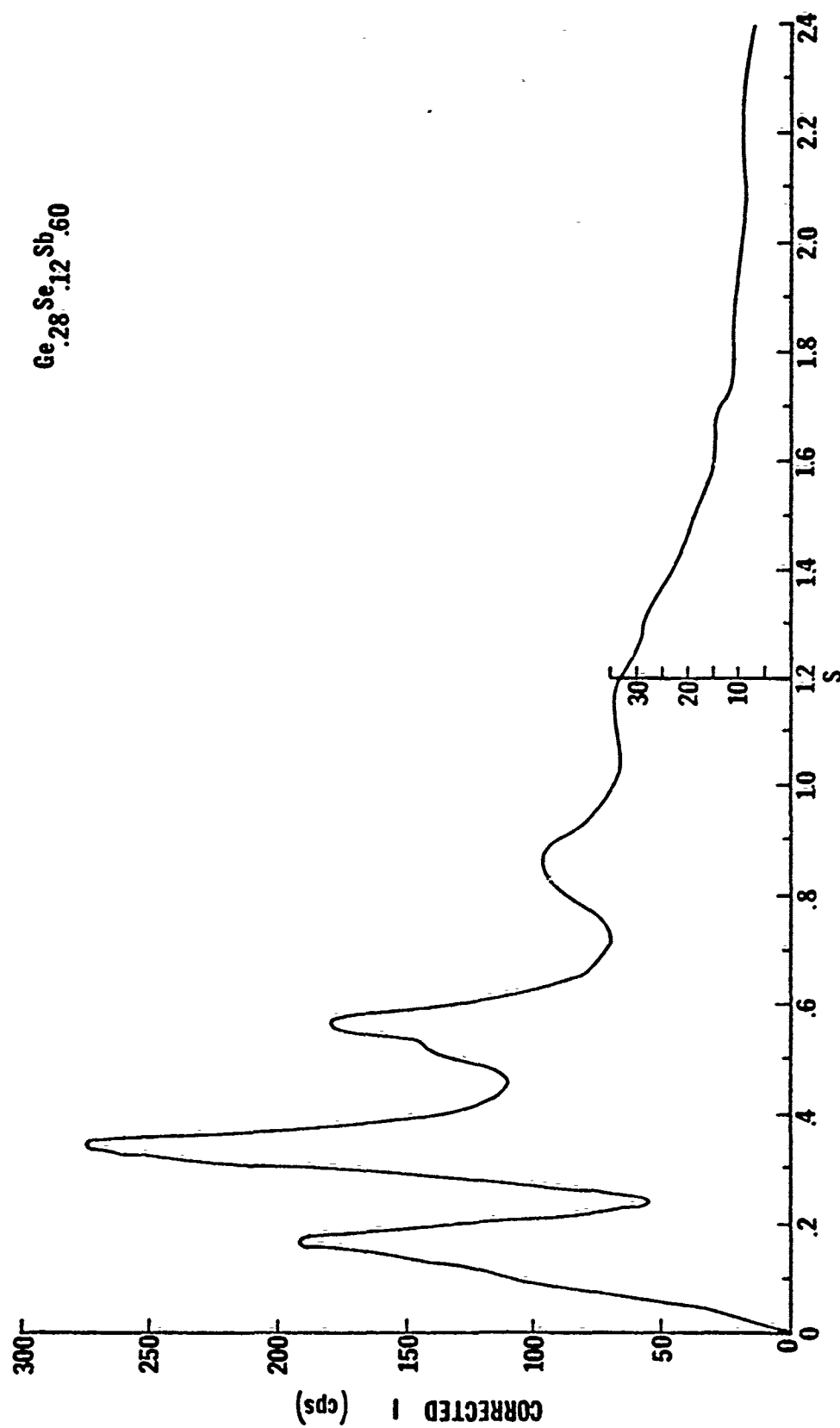


Fig. 5. X-ray intensity vs. scattering angle for $\text{Ge}_{28}\text{Se}_{12}\text{Sb}_{60}$.

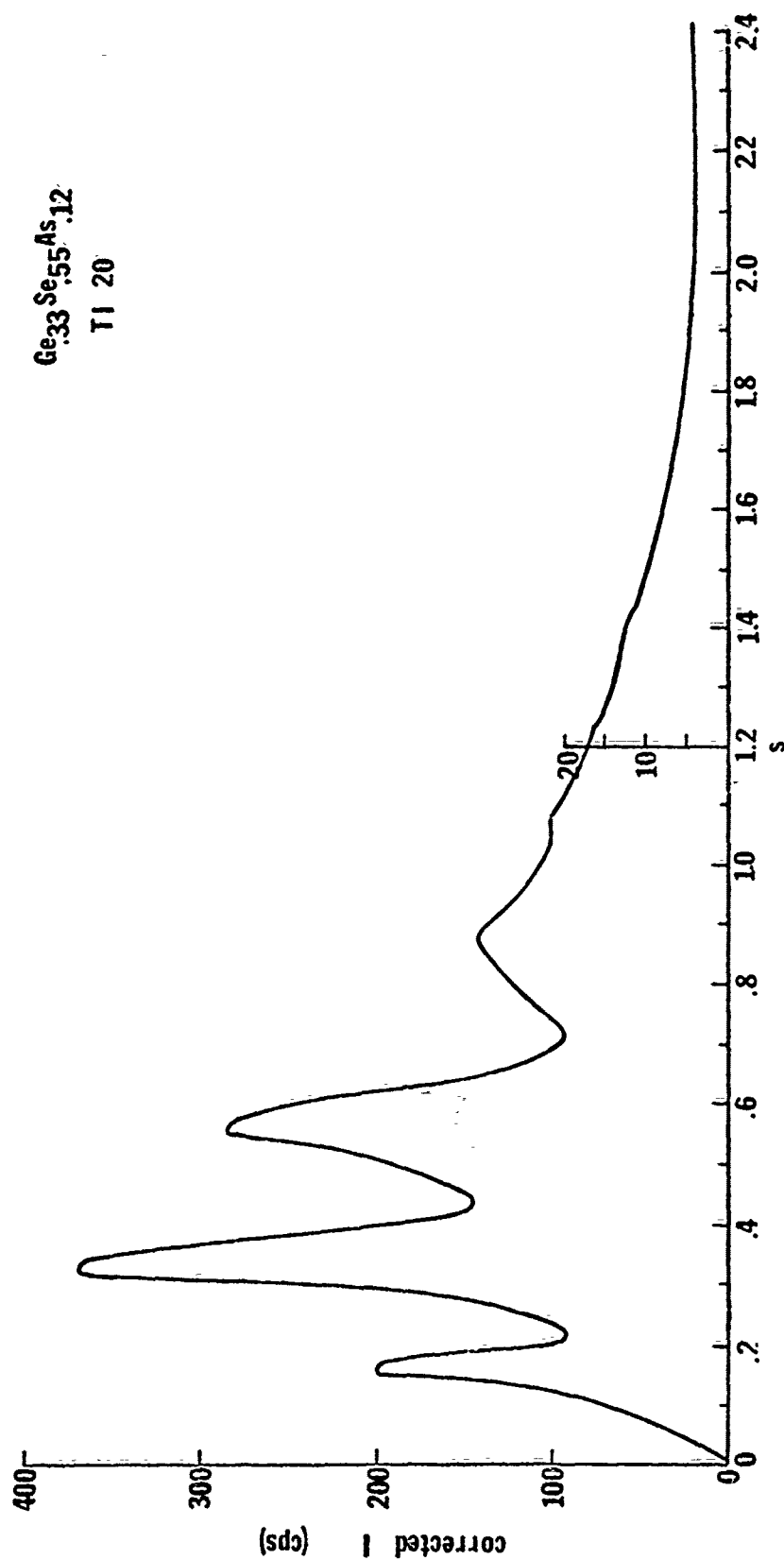


Fig. 6. X-ray intensity vs. scattering angle for $\text{Ge}_{33}\text{Se}_{55}\text{As}_{12}$ (TI-20).

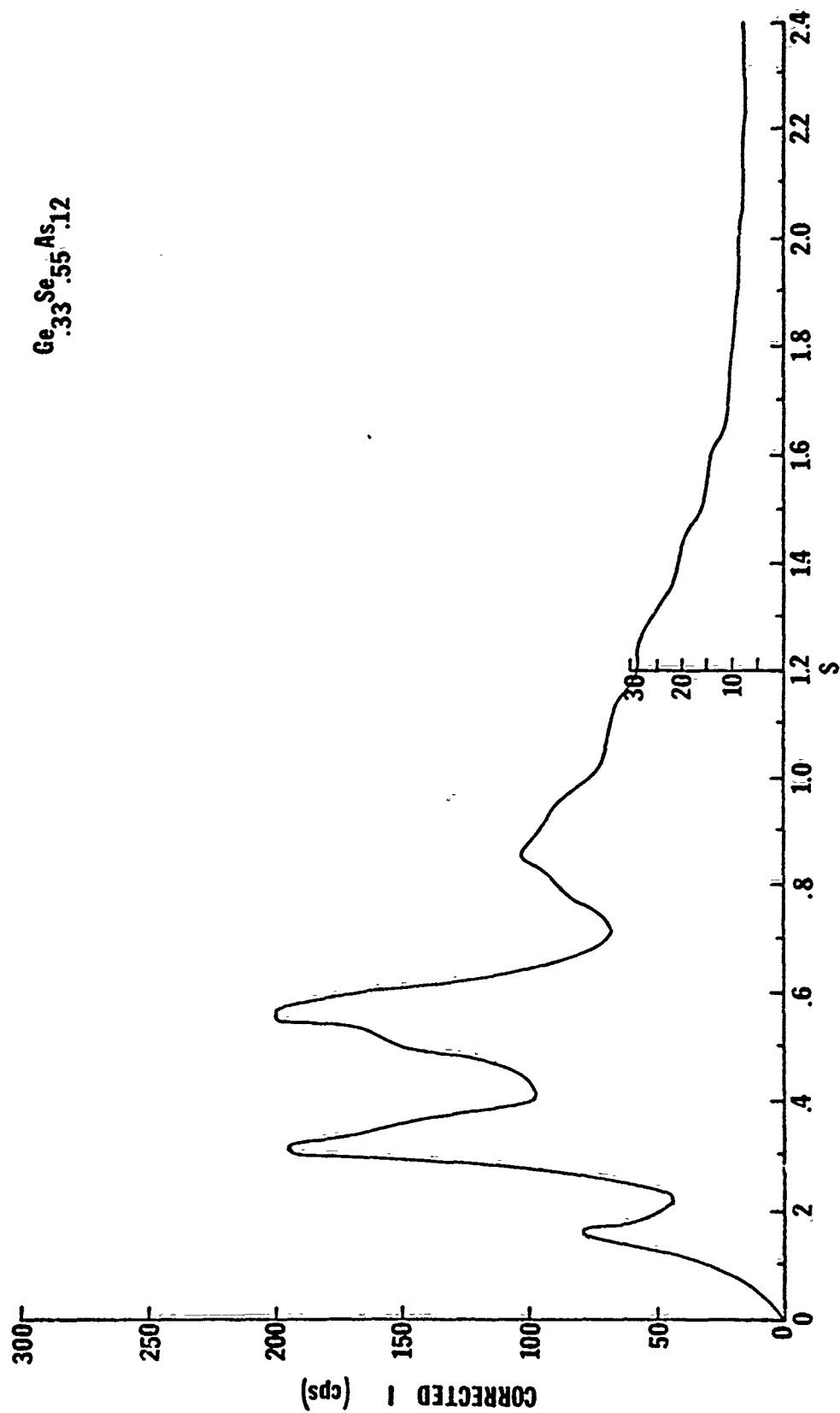
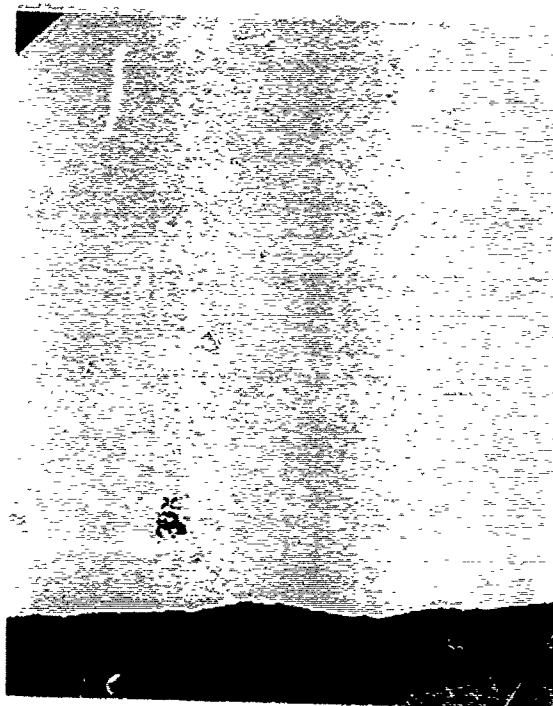
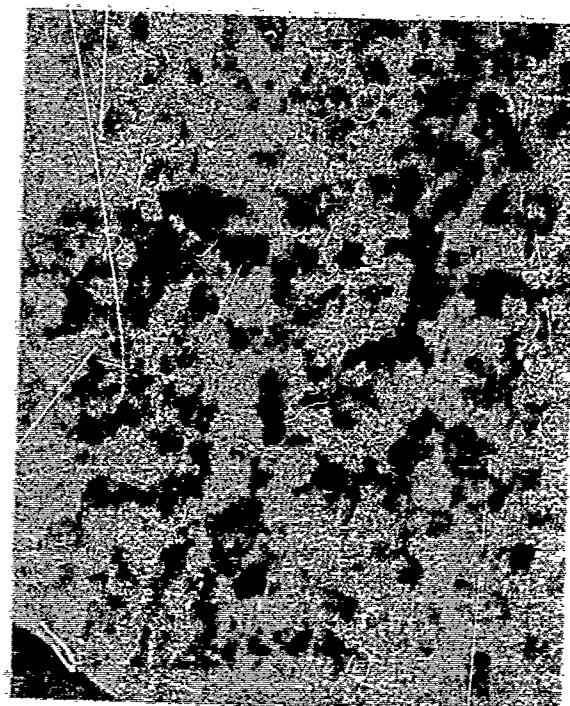


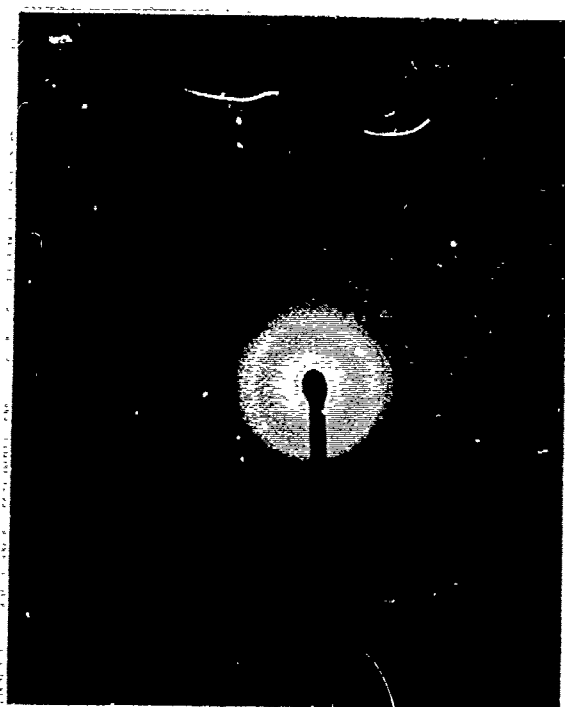
Fig. 7. X-ray intensity vs. scattering angle for $\text{Ge}_{.33}\text{Se}_{.55}\text{As}_{.12}$ (University of Florida).



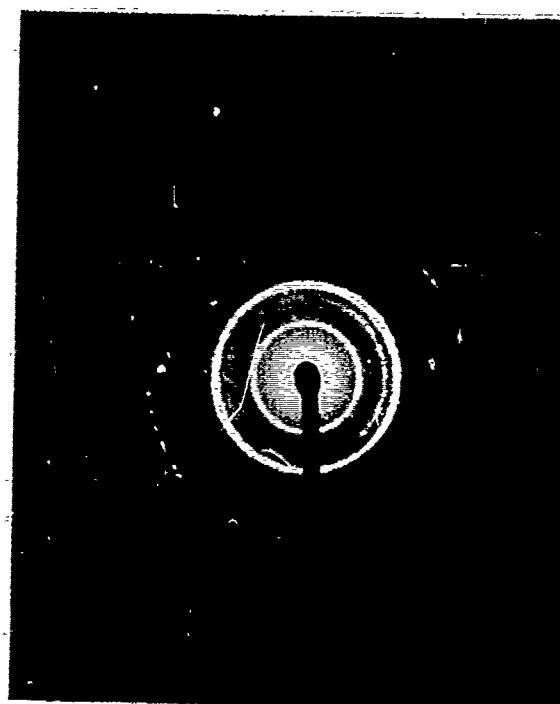
(a)



(c)



(b)



(d)

Fig. 8. Electron micrographs of GeTe₂ films before and after heat treatment.

the bulk form. Electron microscopy studies in this laboratory show that Se based glasses prepared as thin films also are monophasic to a fine scale, ca. 100Å, for an extremely wide range of compositions [8], [12]. Preliminary scanning calorimetry results from our laboratory indicate that gross phase separation does not occur in Se based glasses in the bulk form as well.

To summarize, it is necessary to know the structure of glasses if one is to make a systematic evaluation of their properties. Chalcogenide glasses have potential both for bulk windows and as protective coatings for alkali halide windows; several candidate materials for both application have so far been shown in this study to be structurally homogeneous to a very fine degree. Material homogeneity, of course, greatly simplifies the interpretation of optical and thermal data.

VI. Infrared Behavior of Glassy Selenium

In order to evaluate the purity of the selenium and the processing used to make the chalcogenide glasses, high purity Se samples were vacuum melted in Pyrex tubes. Samples of thickness 2.5mm were cut from the tubes and ground and polished using the procedure described. Infrared spectra were taken of the samples using a Beckman IR10 spectrophotometer. A plot of absorption vs. wavelength is given for three Se samples in Figure 9. The infrared spectra obtained are similar to the spectra presented by Lacourse and Twaddell [7] for pure de-oxygenated glassy Se in which the oxygen content was less than 2 ppm. No absorption bands due to the presence of SeO were detected. The bands at 13.7μm and 20.3μm are intrinsic to glassy Se. The major cause of infrared absorption in the Se samples examined in this laboratory was the presence of microvoids. Consequently this study showed that high purity glassy selenium prepared by our processing methods does not yield Se-O absorption bands.

VII. Infrared Behavior of Chalcogenide Glasses

The infrared absorbance was measured in the range 6 to 16μm for samples of the following compositions: (1) GeSe₄, (2) GeSeAs, (3) Ge₂Se₃As, (4) Ge₃₃Se₅₅As₁₂, (5) Ge₃Se₅As, and (6) Ge₂₈Sb₁₂Se₆₀ (obtained from Texas Instruments). Ge₃Se₅As samples containing 0.15 at. % Ti, 0.15 at. % Zr, and 0.36 at. % Ti, respectively, were also examined.

The absorption spectra of all samples of the first five compositions listed above exhibited a large absorption band around 7.8μm and a broad absorption band with a maximum lying between 11 and 14μm. Since these two bands were found in the

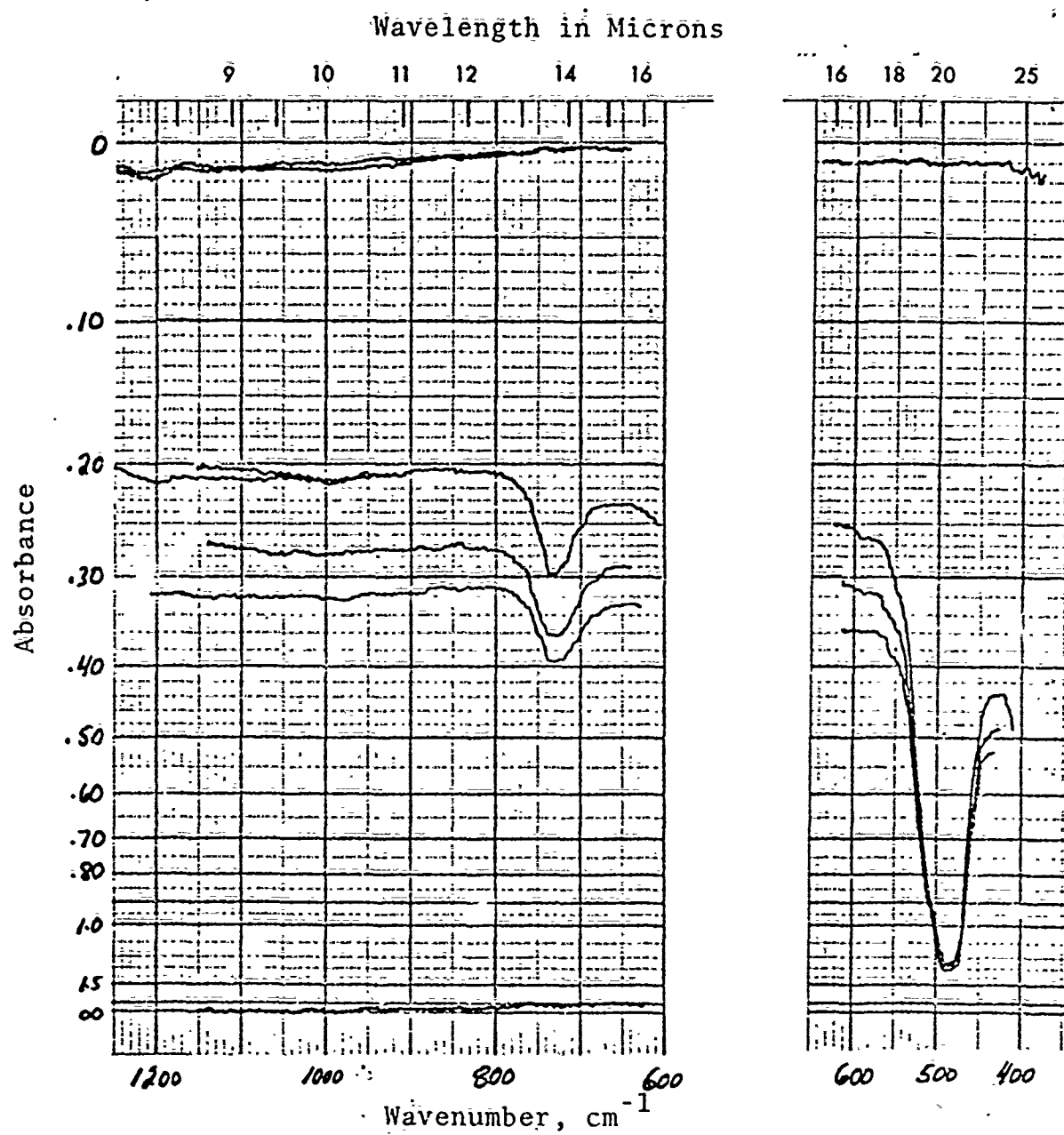


Fig. 9. Absorbance vs. wavelength for three Se samples.
(upper straight curve: machine base line)

GeSe glass as well as in the Ge-Se-As glasses, it appears that these bands are not caused by the presence of arsenic. In his investigation of the infrared absorption of Ge-Se glasses, Hilton [13] attributed the presence of an absorption band at $13\mu\text{m}$ to Ge-O bonds. Hilton also obtained an absorption band at $8\mu\text{m}$, but did not offer an explanation for its origin. It therefore seems probable that the primary factor limiting the transmittance at $10.6\mu\text{m}$ in the Ge-Se-As glasses is the presence of Ge-O bonds.

$\text{Ge}_3\text{Se}_5\text{As}$ was found to have the lowest absorbance at $10.6\mu\text{m}$ (942 cm^{-1}) of the glasses made in this laboratory. Two samples were made of pure $\text{Ge}_3\text{Se}_5\text{As}$, one in a Vycor tube and one in a quartz tube. Both samples had an absorbance of 0.58 at $10.6\mu\text{m}$. Figure 10 shows the absorption spectrum for $\text{Ge}_3\text{Se}_5\text{As}$.

In an effort to reduce the number of Ge-O bonds in the glass and hence improve its transmittance, the effect of adding a getter to $\text{Ge}_3\text{Se}_5\text{As}$ was investigated. The addition of 0.15 at.% Zr to the system did not result in a significant change in the absorbance. Addition of 0.15 at.% Ti, however, resulted in an absorbance at $10.6\mu\text{m}$ of 0.36, a considerable decrease from the absorbance obtained from the pure glass. The absorption spectrum for this sample is shown in Figure 11. Addition of 0.36 at.% Ti resulted in an absorbance of 0.43 at $10.6\mu\text{m}$. Expiration of the contract terminated experiments to determine the atomic percentage of Ti which will yield the maximum decrease in the absorbance of $\text{Ge}_3\text{Se}_5\text{As}$.

As discussed by Lezal and Srb [14], contamination of the chalcogenide glasses with oxygen can result both from the presence of oxygen impurities in the elements used to synthesize the glass and from diffusion of oxygen from the reaction tube into the reacting system during the synthesis. At the termination of the contract initial experiments were underway to deoxidize Ge by vacuum melting in a highly pure graphite crucible prior to glass synthesis. The synthesis itself was to be carried out in the graphite crucible under controlled atmospheric conditions. Only very limited success was achieved in the time available.

Samples of thickness 2.5 mm were cut and polished from a piece of $\text{Ge}_{28}\text{Sb}_{12}\text{Se}_{60}$ glass obtained from Texas Instruments. A typical absorption spectrum obtained from this glass is shown in Figure 12. The absorbance at $10.6\mu\text{m}$ for this sample was found to be 0.22. Figure 13 gives a plot of absorbance A vs. refractive index n for various values of αx , where α is the absorption coefficient and x is the sample thickness, assuming no scattering of incident radiation. This plot indicates that for a $\text{Ge}_{28}\text{Sb}_{12}\text{Se}_{60}$ ($n \approx 2.6$) sample with $\alpha = 0$, one would expect an absorbance of $A \approx 0.18$. The fact that

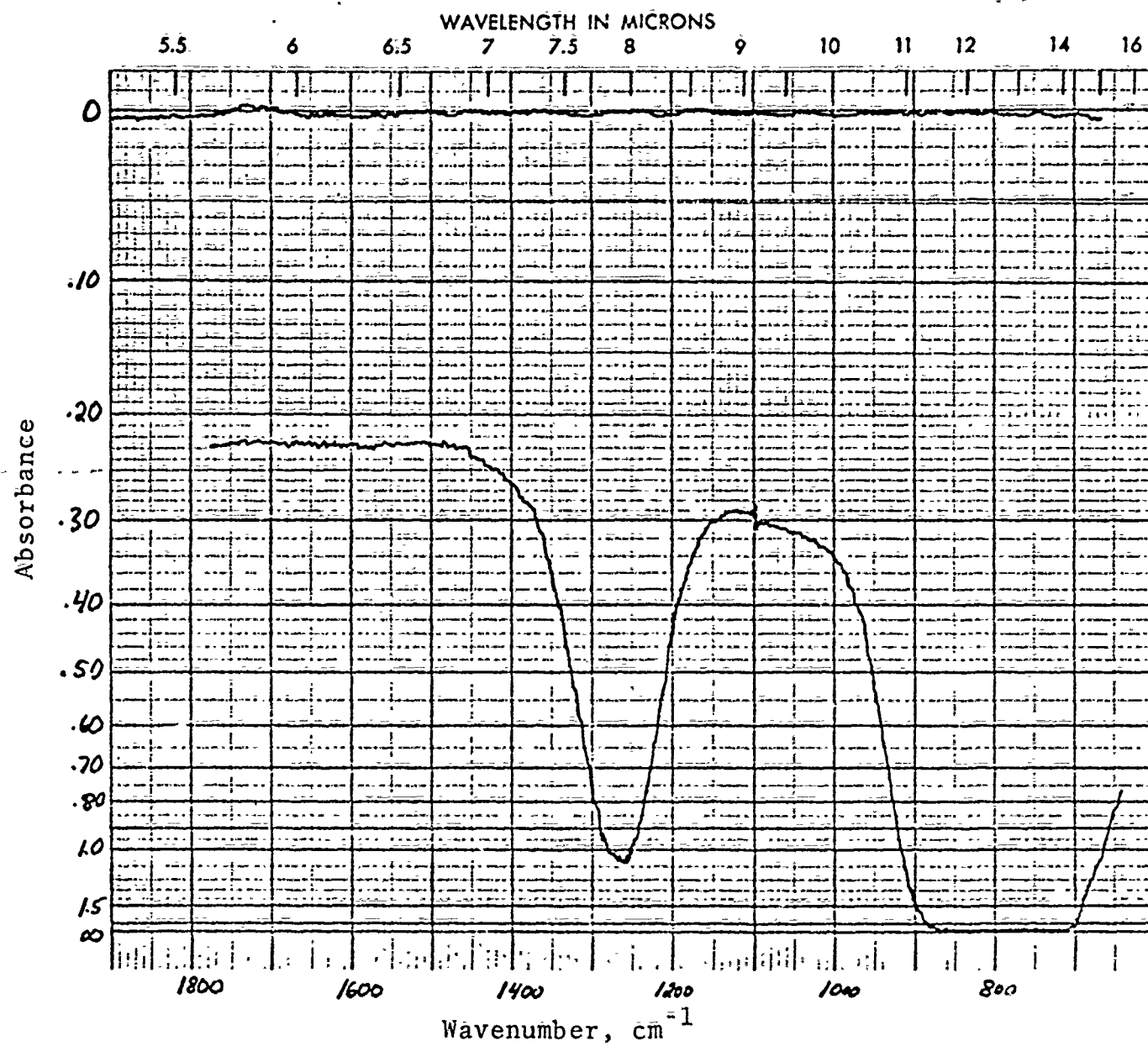


Fig. 10. $\text{Ge}_3\text{Se}_5\text{As}$ absorption spectrum.

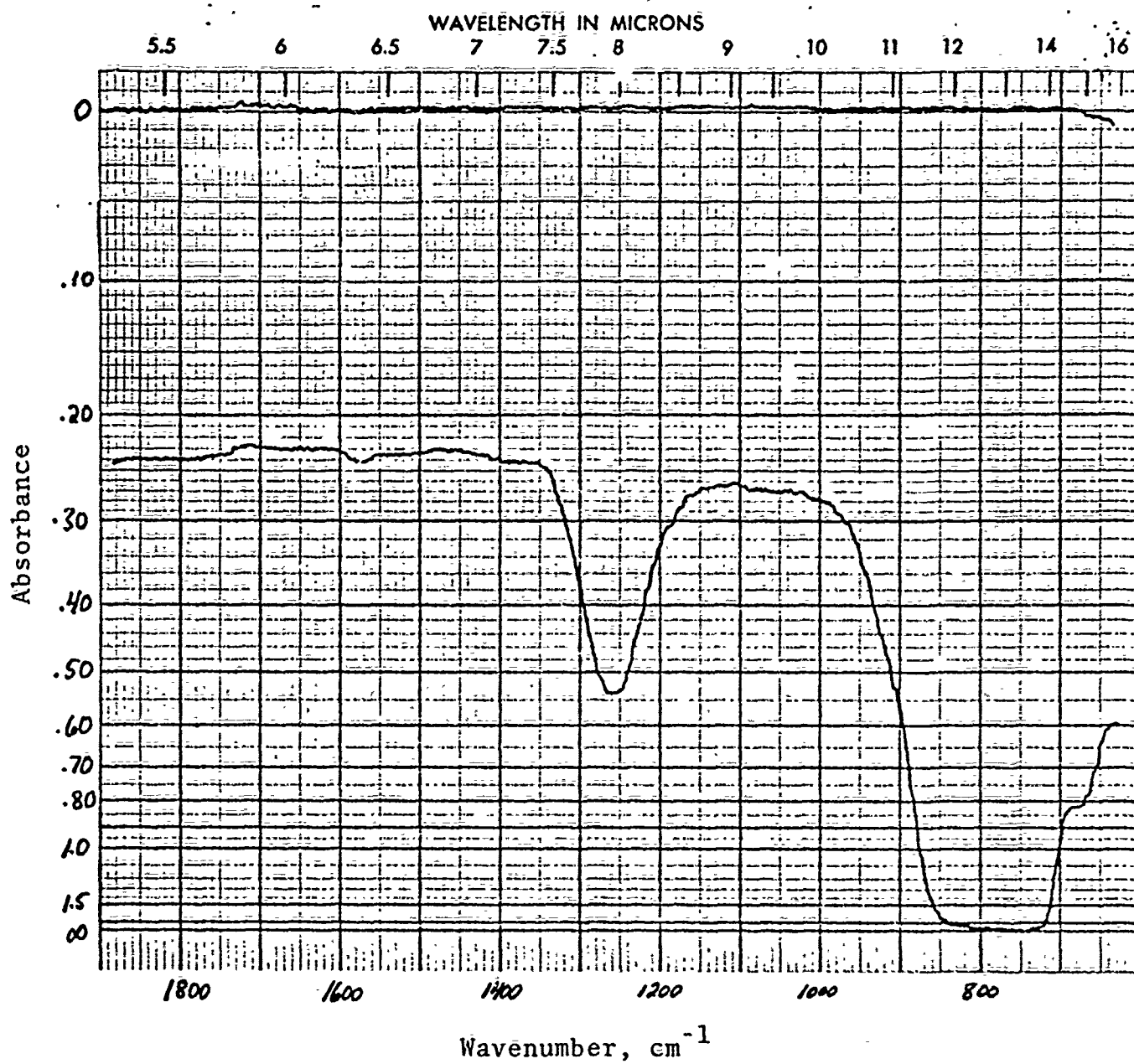


Fig. 11. Absorption spectrum of $\text{Ge}_3\text{Se}_5\text{As} + 0.15\% \text{Ti}$.

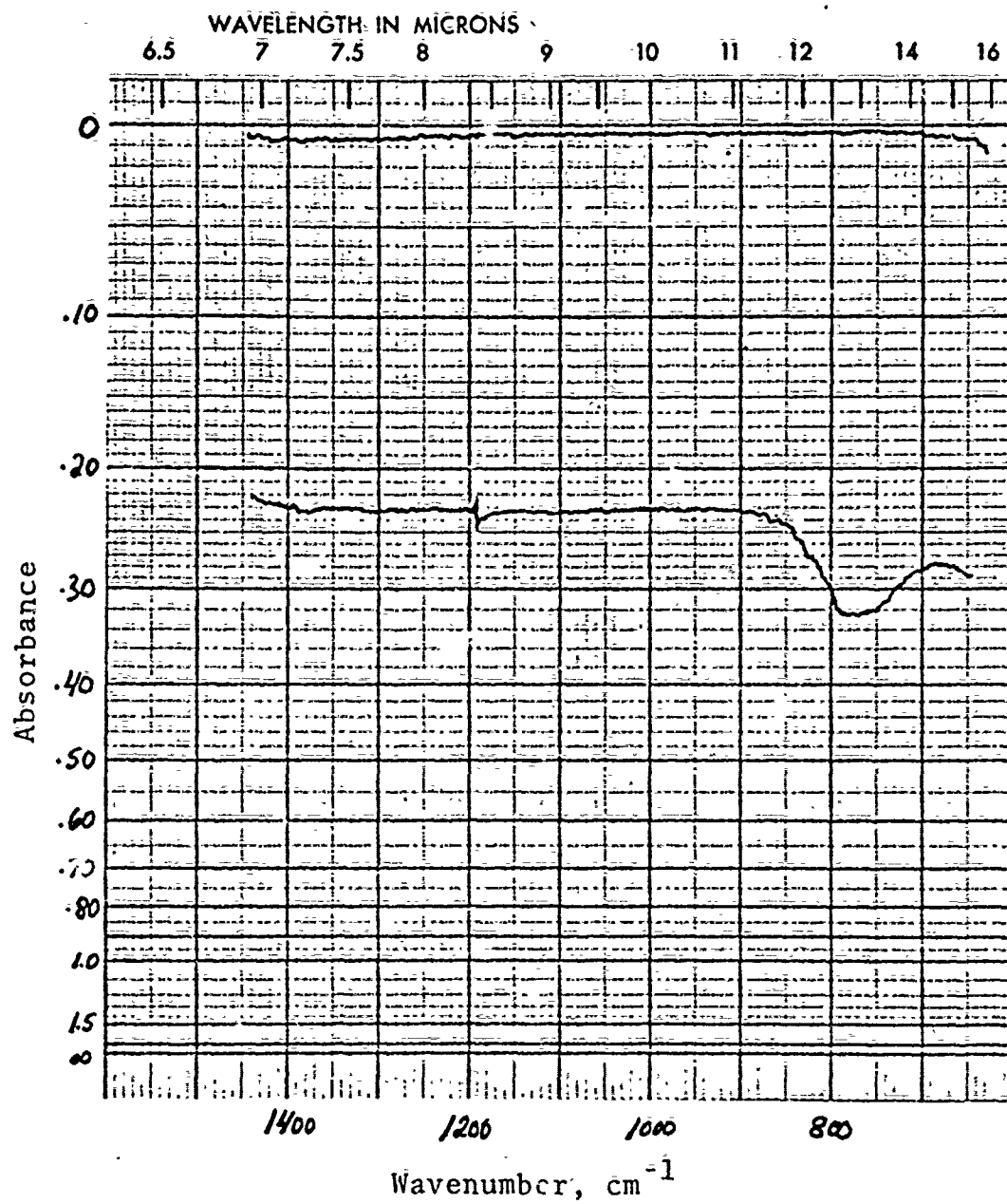


Fig. 12. Absorption spectrum of $\text{Ge}_{28}\text{Sb}_{12}\text{Se}_{60}$ (TI-1173 glass).

this value is quite close to the measured absorbance of 0.22 gives strong indication that the α for this sample is quite small.

VIII. Thermal Treatment Studies of Chalcogenide Glasses

The potential importance of thermal treatment of laser window glasses was discussed by the authors in the conference on High Power Laser Windows [15]. A copy of this paper is included as appendix A.

The objective of this phase of the study is to investigate the influence of thermal treatment on properties relevant to the infrared transmitting ability, structural stability, and thermal stability of chalcogenide glasses. Work so far has concentrated on the same relatively simple compositions in the Ge-Se-As system mentioned previously. Texas Instruments TI-1173 glass ($\text{Ge}_{28}\text{Sb}_{12}\text{Se}_{60}$) and TI-20 glass ($\text{Ge}_{33}\text{Se}_{55}\text{As}_{12}$) also were studied because of their present use as infrared window materials. Preliminary results were previously reported [15]. The following sections present more detailed studies.

A. X-ray analysis

Texas Instruments 1173 glass ($\text{Ge}_{28}\text{Sb}_{12}\text{Se}_{60}$) was subjected to thermal treatment for varying lengths of time to determine the influence of long term heat treating on optical properties. Samples were heated for as long as 340 hours at 300°C; this temperature was chosen to be just below that for the glass transition. No change in the amorphous x-ray spectrum was observed, even for the maximum thermal exposure. Figure 14 is a representative x-ray scan from one of these experiments. Optical absorption measurements on samples subjected to similar heat treatments likewise showed no change.

B. Crystallization studies

This phase of the investigation had as its objective the determination of the glass transition temperature (T_g) and crystallization temperature (T_c) for several amorphous chalcogenides as a function of composition, impurity concentration, method of preparation and degree of heat treatment.

T_g 's and T_c 's for several compositions in the Ge-Se-As ternary were determined in the range 300 to 773°K with a Perkin-Elmer DSC-1B Differential Scanning Calorimeter. Scanning rates from 2-1/2 to 20 degrees/minute were used. The baseline drift observed for some compositions has been attributed to sample volatility at temperatures above 400°K. Use of a recently acquired PE accessory sample sealing kit for encapsulating volatile samples would eliminate this drift.

SAMPLE 5

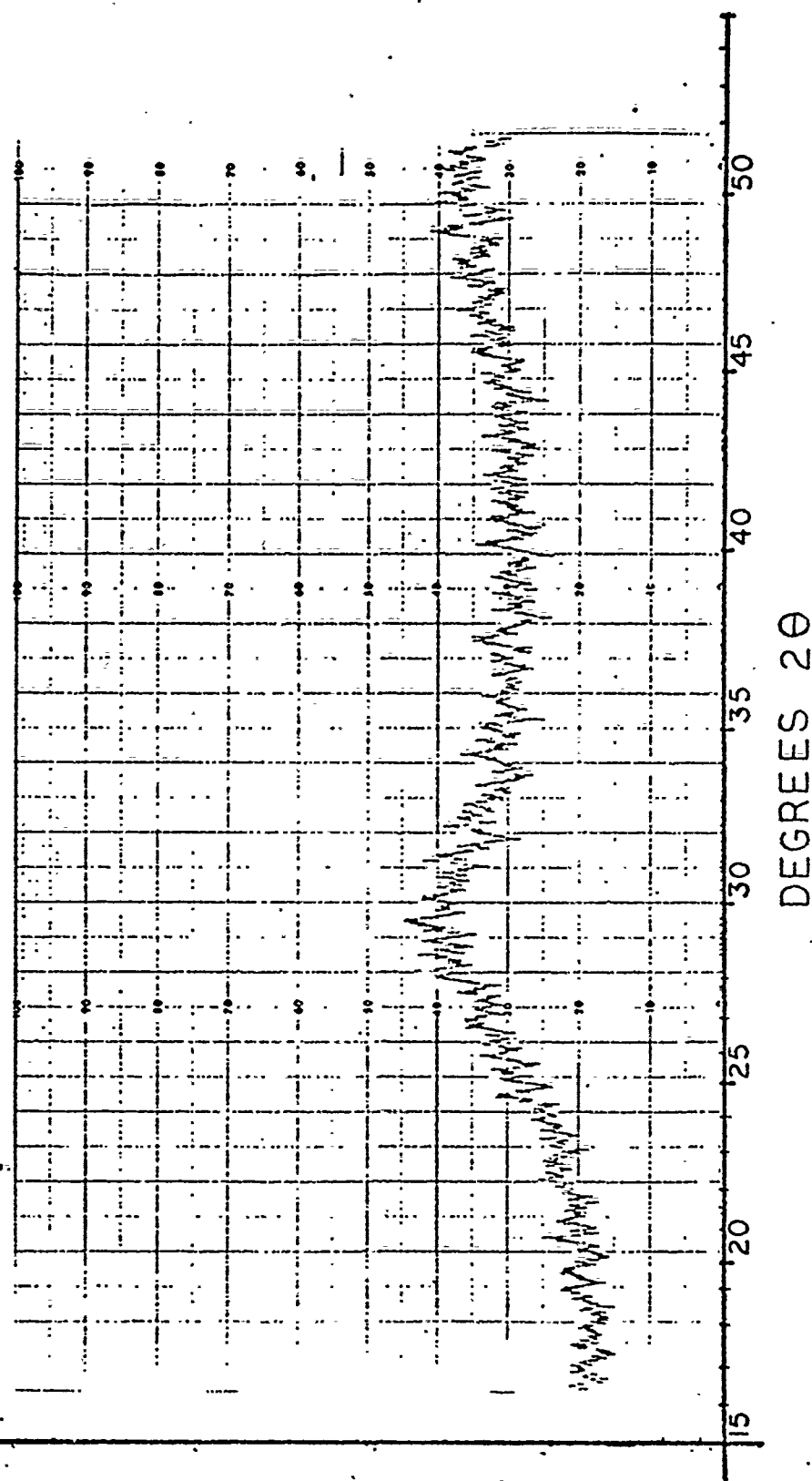
100 Scale Factor

40 KV 15 MA

TI 1173

Heat Treat 60 hrs at 300°C

INTENSITY

Fig. 14. X-ray spectrum of heat treated $\text{Ge}_{28}\text{Sb}_{12}\text{Se}_{60}$ glass.

Preliminary studies on the compositions GeSeAs , $\text{Ge}_{33}\text{Se}_{55}\text{As}_{12}$, $\text{Ge}_3\text{Se}_5\text{As}$, $\text{GeSe}_{2.9}\text{As}_{0.1}$, $\text{GeSe}_{1.5}$ and $\text{Ge}_{28}\text{Sb}_{12}\text{Se}_{60}$ were performed. All but $\text{GeSe}_{1.5}$ do not crystallize for repeated scans from 300 to 773°K, while exhibiting reproducible Tg's in the range 550 to 700°K.

$\text{GeSe}_{1.5}$ shows a Tg of about 625°K which is independent of scan rate and which is reproducible from sample to sample. The most interesting feature, however, is the apparent two-stage crystallization which occurs at higher temperatures. A small, broad exothermic peak centered at 714°K is overlapped by a larger, sharper one centered at 745°K. (Figure 15 is a scan which illustrates this effect.) Doubling the scan rate to 20 degrees/minute shifts the onset of the crystallization peaks to slightly higher temperatures.

In a related experiment, retention of a sample of $\text{GeSe}_{1.5}$ at 690°K for 15 minutes before scanning upwards in temperature at 2-1/2 degrees/minute produced single, very broad peak centered at 728°K; apparently the scan rate was too slow to resolve the two peaks seen at higher scan rates. Other experiments were conducted to identify the species crystallizing. Portions of $\text{GeSe}_{1.5}$ were heated in evacuated Pyrex ampoules for varying lengths of time at 723 and 748°K, after which they were quenched and subjected to powder x-ray diffraction analysis. The spectra obtained are complex and peaks obtained have not all been identified. Tentative results are that a two-stage process also is observed; that Se is one of the first crystallizing species; and that if the $\text{GeSe}_{1.5}$ is heated long enough only GeSe and GeSe_2 are present. The details of the crystallization behavior remain to be worked out as is the relation of these processes to the equilibrium Ge-Se phase diagram.

Earlier in this report it was stated that small amounts of various transition metals were added to $\text{Ge}_3\text{Se}_5\text{As}$ in an attempt to lower the IR absorption. The influence of these additions on the thermal stability of the glass was investigated by Differential Scanning Calorimetry. Samples of $\text{Ge}_3\text{Se}_5\text{As}$ with additions of 0.36 wt. % Ti, 0.15 wt.% Ti or 0.15 St.% Zr were run in the manner described above. In all cases the Tg's were unchanged from those observed in the same glass with no added metal; in no case was any crystallization observed even when the sample was repeatedly cycled between 450 and 774°K. We must conclude, then, that within the limits of these experiments the thermal stability of amorphous $\text{Ge}_3\text{Se}_5\text{As}$ is unaffected by the addition of small amounts of Ti or Zr.

The effect of cyclic heat treatment on the thermal stability of $\text{Ge}_{28}\text{Sb}_{12}\text{Se}_{60}$ glass was investigated with the DSC by scanning from 300 to 773°K and back to 300°K for five complete cycles. The scan rate was either 10 or 20 degrees/minute. Figure 16 is a portion of the initial scan taken at 10 degrees/minute. Figure 17 illustrates the upward scan on the

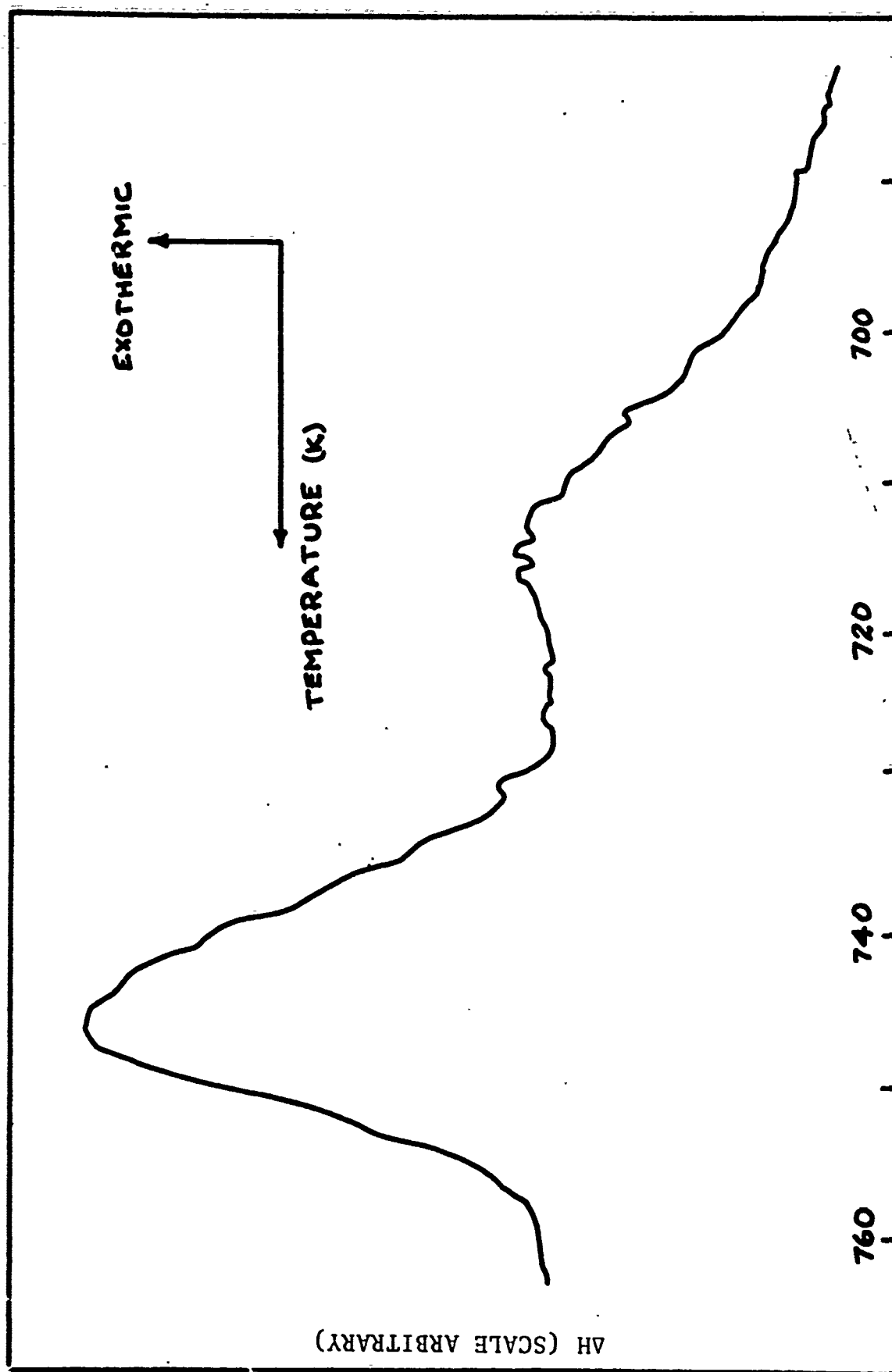


Fig. 15. Differential Scanning Calorimeter scan of two-stage crystallization in $\text{GeSe}_{1.5}$.

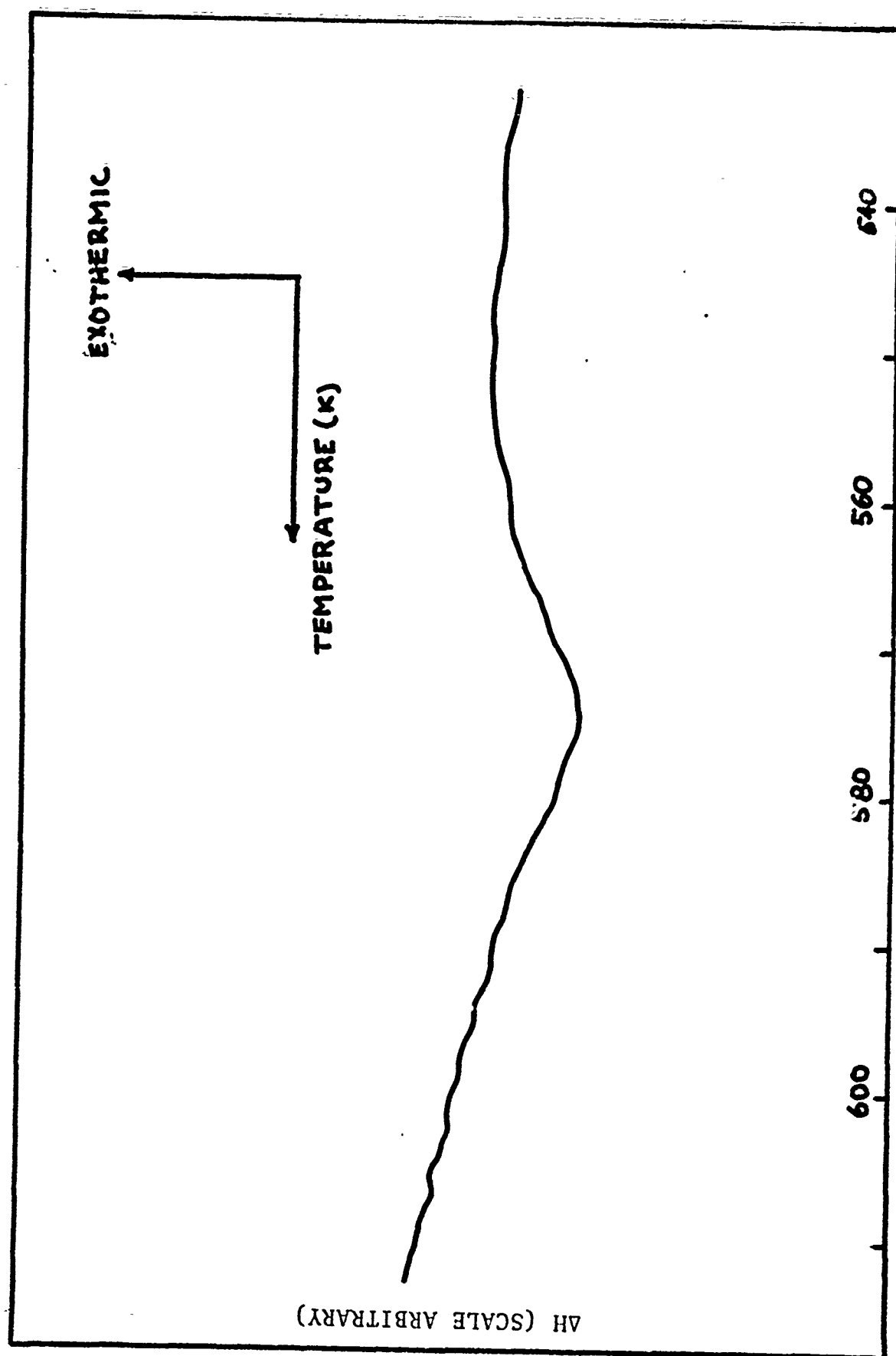


Fig. 16. Differential Scanning Calorimeter scan of $\text{Ge}_{28}\text{Sb}_{12}\text{Sc}_{60}$, 10 deg/min, first thermal cycle.

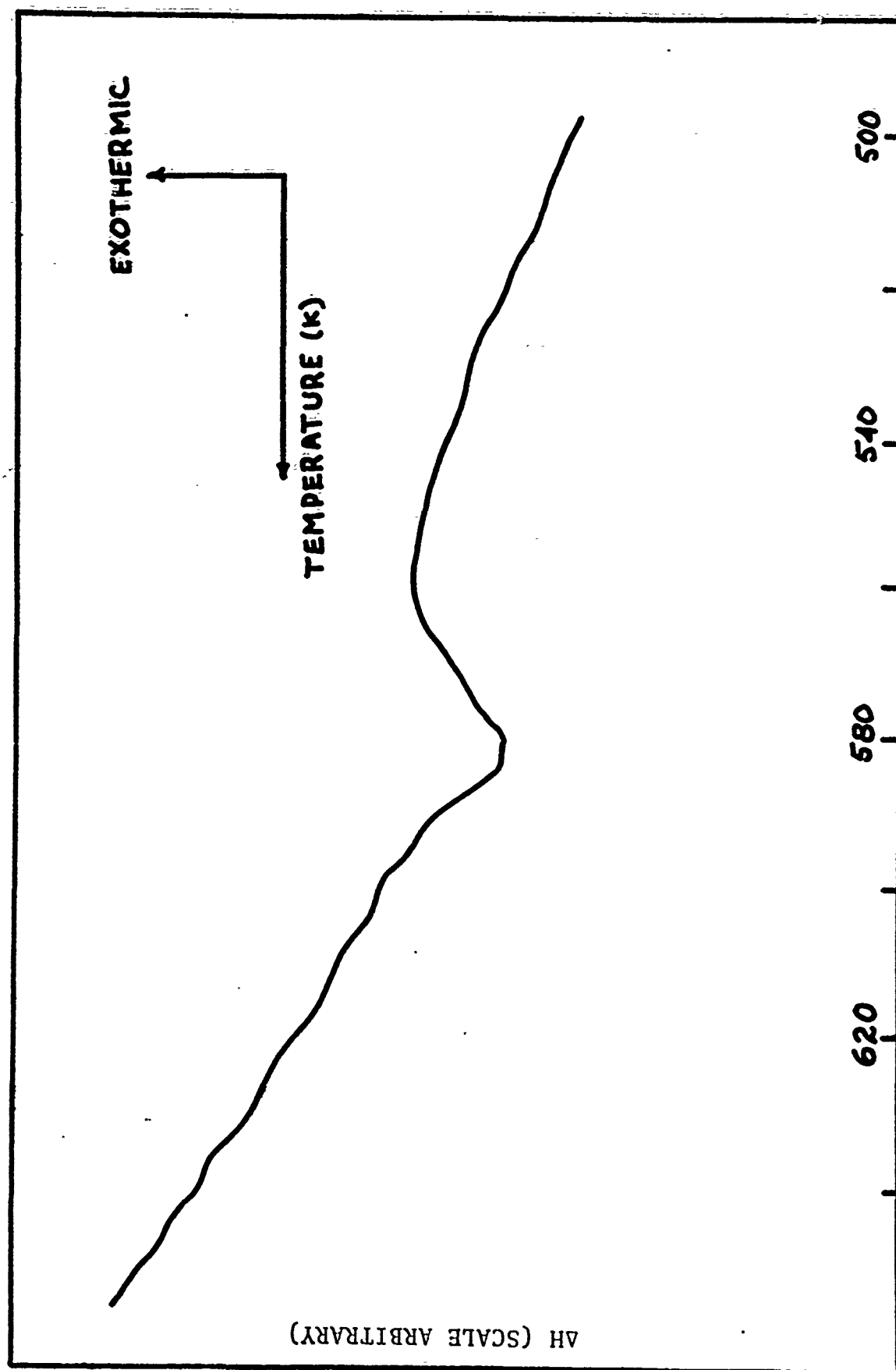


Fig. 17. Differential Scanning Calorimeter scan of $\text{Ge}_{28}\text{Sb}_{12}\text{Se}_{60}$, 20 deg/min, fifth thermal cycle.

fifth cycle taken at 20 degrees/minute. The T_g is unaltered by the repeated cycling and no crystallization is observed.

C. Density variations

Densities of a series of TI-20 and TI-1173 glasses which had been heat treated for varying lengths of time were determined by the Archimedes method using CCl_4 as the density fluid. Table II shows the results of these measurements; each entry in the table represents four to eight individual determinations. As can be seen from the table, there is no significant density change for TI-1173 for heat treatment times exceeding 340 hours at $300^\circ C$, while the same conditions produce small but definite changes in the density of TI-20 glass. As stated above, x-ray determinations on portions of these identical samples showed no detectable crystallization. The implication of these results is, of course, that TI-1173 is thermally more stable than TI-20, although both glasses are quite resistant to thermally induced changes.

D. Mechanical property studies

Samples of TI-20 and TI-1173 glasses prepared for mechanical property measurements were heat treated simultaneously with the density and x-ray samples. Properties studied were surface tensile strength, bulk tensile strength and micro-hardness. Surface tensile strength was measured by the conventional three-point bending technique illustrated diagrammatically in Table III. The 5,000-6,000 psi modulus of rupture values obtained compare quite favorably with those of soda-lime-silica glasses obtained under similar conditions. [16] Table III shows the results of these tests. The load was applied to surfaces optically polished thereby simulating the loading of a laser window. A 0.2 inch/minute strain rate was used with an Instron testing machine. As can be seen, the rather wide scatter in the data prevents any definite conclusions about the effect of heat treatment from being made. This degree of scatter is not unusual for such tests on brittle ceramic materials. However, a trend is certainly suggested that prolonged surface treatment deteriorates the modulus of rupture of these glasses. Since vaporization from the glasses occurred during the long heat treatment the strength decrease may in part be due to alteration of the glass surface.

Bulk tensile strengths were measured by performing diametral compression tests [17] on approximately 0.250 inch diameter cylinders of TI-20 and TI-1173. The samples were obtained by diamond core drilling commercial IR glass window blanks. These results are presented in Table IV. As with the three-point loading experiments, there is considerable scatter in the data so that only general trends can be inferred. The limited amount of heat treatment for TI-1173 seems to produce no change while considerably greater heat treatment seems to produce a slight decrease in tensile strength for TI-20 glass.

Table II
Density Determinations

	Heat Treatment (hours)	Average Density (95% C.I.)
TI-1173	0	4.6617 ± .0044 g/cc
	48	4.6453 ± .0008
	96	4.6339 ± .0054
	213	4.6419 ± .0042
	344	4.6337 ± .0108
TI-20	0	4.3994 ± .0006 g/cc
	92	4.3971 ± .0004
	168	4.4043 ± .0006
	337	4.4236 ± .0020

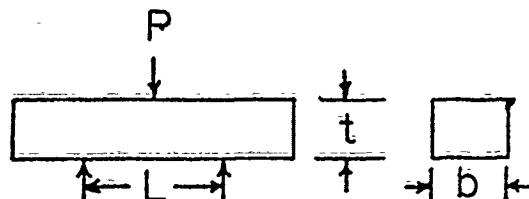
$$95\% \text{ C.I.} = \frac{2 \text{ SD}}{\sqrt{n}}$$

where SD = standard deviation

n = number of observations

Table III
Surface Tensile Strength by Three-Point Loading

Surface tensile stress



$$\sigma_s = \frac{MC}{I} \quad M = \frac{1}{2} LP \quad C = \frac{1}{2} t$$

$$I = \frac{bh^3}{12} \quad L = 0.75''$$

$$\sigma_s = \frac{3LP}{bt^2}$$

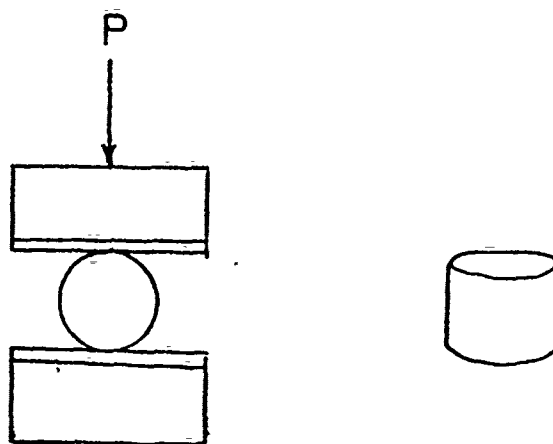
Trial Number	Maximum Loading	t	b	Tensile Strength
TI-20, no heat treatment				
1	66 lbs.	.250	.255	9,317 psi
2	60	.250	.251	8,605
3	35	.250	.248	5,080
4	30.5	.252	.247	4,375
5	42.5	"	.253	5,952
6	55.5	"	.251	7,834
7	48	"	.250	6,803
8	59	"	.251	8,328
9	43	"	.253	6,022
Average				6,924±1,066 psi
TI-20, 337 hours at 300°C				
1	24	.252	.251	3,388
2	38	.252	.250	5,385
3	43	.252	.250	6,094
Average				4,955±1,320 psi
TI-1173, no heat treatment				
1	23	.250	.252	3,259

Table IV
Diametral Compression Tests

$$\sigma = \frac{2P}{\pi Dt}$$

where P = load
D = diameter
t = length

	Heat Treatment (hours)	Average Tensile Strength
TI-1173	0 (4 samples)	3,316 ± 1,106 psi
TI-20	0 (6 samples)	2,905 ± 512 psi
	337 (3 samples)	2,065 ± 292



Microhardness was determined with a Knoop diamond indenter using a 10 g load applied for ten seconds on optically polished surfaces. Results are presented in Table V; each entry is the average of at least ten separate determinations. The precision of these measurements is considerably greater than that resulting from the three-point bending and diametral compression tests. As Table V shows, the microhardness of both TI-20 and TI-1173 are independent of heat treatment times up to 337 hours at 300°C. The microhardness value of TI-1173 is lower than the 150 value previously reported by Hilton for the same composition ($\text{Ge}_{20}\text{Sb}_{12}\text{Se}_{60}$). [18] Likewise, our 135 hardness value for the TI-20 glass is lower than the 171 value reported by Hilton [19]. In considering the wide scatter in hardness values for Chalcogenide glasses [20] this variation is not atypical. The thermal treatment results reported herein show that variations in hardness are not due to differences in thermal history but are related to composition or perhaps surface polishing methods.

The inescapable conclusion from this study of mechanical properties of TI-20 and TI-1173 is that these two compositions are extremely stable glasses. For even the extended heat treatments reported here the materials are x-ray amorphous. Density variations in TI-20 for 337 hours at 300°C possibly indicate incipient crystallization while TI-1173 shows no such change. However, as discussed above, tensile strength and microhardness measurements show at most only minimal change. These findings, coupled with their known low optical absorption at 10.6 μm , suggest that TI-20 and TI-1173 are worthy of further testing of their suitability as high power laser window materials.

IX. Coated Polycrystalline Alkali Halides

A. Nature of the problem

The alkali halides are candidates for infrared transmitting window materials, because of their low absorption coefficients ($2.7 \times 10^{-3} \text{ cm}^{-1}$ for KCl, $5 \times 10^{-5} \text{ cm}^{-1}$ for KBr at 10.6 μm) [21]. However, if these materials are to find wide use in applications requiring the transmission of large power densities, ways must be found to improve their rather poor mechanical properties. For example, the critical fracture stress of single crystal NaCl is only 570 psi, while that for KCl is 640 psi; these contrast with a value of 65,000 psi for single crystal Al_2O_3 . [22]

The values quoted above are much lower than those predicted for a perfect crystal, in which case the fracture stress, σ_m , is given by [15]

$$\sigma_m \approx \frac{2\gamma E}{a} \approx E/10 \sim 10^6 \text{ psi}$$

Table V
Microhardness Data

	Heat Treatment (hours)	Average Knoop Hardness (95% C.I.)
TI-1173	0	126 ± 12 kg/mm ²
	10	122 ± 5.4
	48	131 ± 7.2
	60	123 ± 7.4
	96	124 ± 5.3
TI-20	0	135 ± 16 kg/mm ²
	92	138 ± 14
	168	126 ± 7.2
	337	137 ± 8.4

$$95\% \text{ C.I.} = \frac{2 \text{ SD}}{\sqrt{n}}$$

where SD = standard deviation
n = number of observations

for the alkali halides. E = elastic modulus, γ = specific surface energy and a = lattice constant.

One explanation for this discrepancy between actual and experimental fracture stresses was advanced by A. A. Griffith [23]. He argued that fracture occurs at a value lower than that predicted theoretically for a perfect solid due to the presence of small cracks or flaws. Strong stress concentrations occur around these cracks when the solid is stressed, causing the cracks to propagate through the material. Fracture of a crystal requires two steps: initial production followed by propagation of a crack to final fracture.

Empirically, it is found that for many real solids, fracture strength is increased as grain size is decreased [24,25]. Specifically,

$$\sigma \propto D^{-1/2} \quad \text{where } D = \text{grain size.}$$

One explanation is that the length of Griffith microcracks is limited to the grain size in fine grain samples and therefore crack propagation is inhibited.

KCl and NaCl are among the materials which, ideally in polycrystalline form, cannot deform plastically without the occurrence of grain boundary rupture [25]. Experimentally, however, some plastic deformation is observed which depends on grain size. This variation results from the fact that plastic deformation occurs only in the vicinity of grain boundary triple lines, and a limited amount of slip may occur within the grains before the stress concentration causes intergranular rupture. The finer the grain size, the greater the crystal volume in the vicinity of triple lines so that the plastic strain before fracture approaches the magnitude of the elastic strain. Thus, as the grain size decreases, the rate of hardening beyond the yield point increases rapidly [25].

A second difficulty with alkali halides is their poor moisture resistance. Any application involving exposure to the atmosphere requires protection of the window against environmental attack. Nonhygroscopic coatings are a solution, but a single outer layer would be susceptible to scratches or abrasion, leading to loss of protection.

B. Polymer Coatings

In the research described, an attempt has been made to combine the strength enhancement of a fine-grained polycrystalline material with the water protection afforded by a hydrophobic intergranular coating. In this approach each crystallite is coated with its own protective layer before

being pressed into a dense, polycrystalline compact. In this way, a breakdown of the coating at any particular point affects only the single crystallite located there, while the rest of the body remains intact under exposure to moisture. It was also thought that by proper choice and thin enough application of the coating, microcrack propagation could be inhibited still further and the mechanical strength improved.

The following criteria were used in the selection of a candidate alkali halide:

- 1) good transmittance at $10.6\mu\text{m}$
- 2) high melting point
- 3) minimization of difference in indices of refraction of alkali halide and coating
- 4) low hygroscopicity
- 5) maximum mechanical strength
- 6) ease of fabrication into a polycrystalline compact.

The criteria for the selection of the coating material were:

- 1) high $10.6\mu\text{m}$ transmittance
- 2) minimum difference between indices of refraction of coating and alkali halide
- 3) high melting point
- 4) good adhesion to alkali halide substrate
- 5) good water resistance
- 6) high mechanical strength
- 7) formation of a layer free from imperfections
- 8) ease of application.

After an extensive literature review of material properties it was decided to restrict the initial experiment studies to coatings of organic polymers. Figure 18 is a plot of index of refraction versus formula weight of the alkali halides; the bands show the range of variation of refractive index for polyethylene and Teflon^R (polytetrafluoroethylene). This graph shows that KCl and NaCl have refractive indices which are closely matched with the range of values exhibited by polyethylene; poorer correspondence exists for the other possible combinations. The fact that KCl is less hygroscopic than NaCl or KBr, and that KCl can be pressed into dense pellets at lower pressure than can NaCl, led to the choice of KCl and polyethylene for the initial studies.

Small crystallites for fabrication into windows were obtained by grinding optical grade single crystal KCl (Harshaw Chemical Company) in an agate mortar and pestle and sieving through a No. 150 Tyler mesh screen. Coatings were made in a variety of ways from high density polyethylene (Marlex TR-885, Phillips Petroleum Company) dissolved in boiling p-xylene. In one technique the KCl crystallites were supported on a wire.

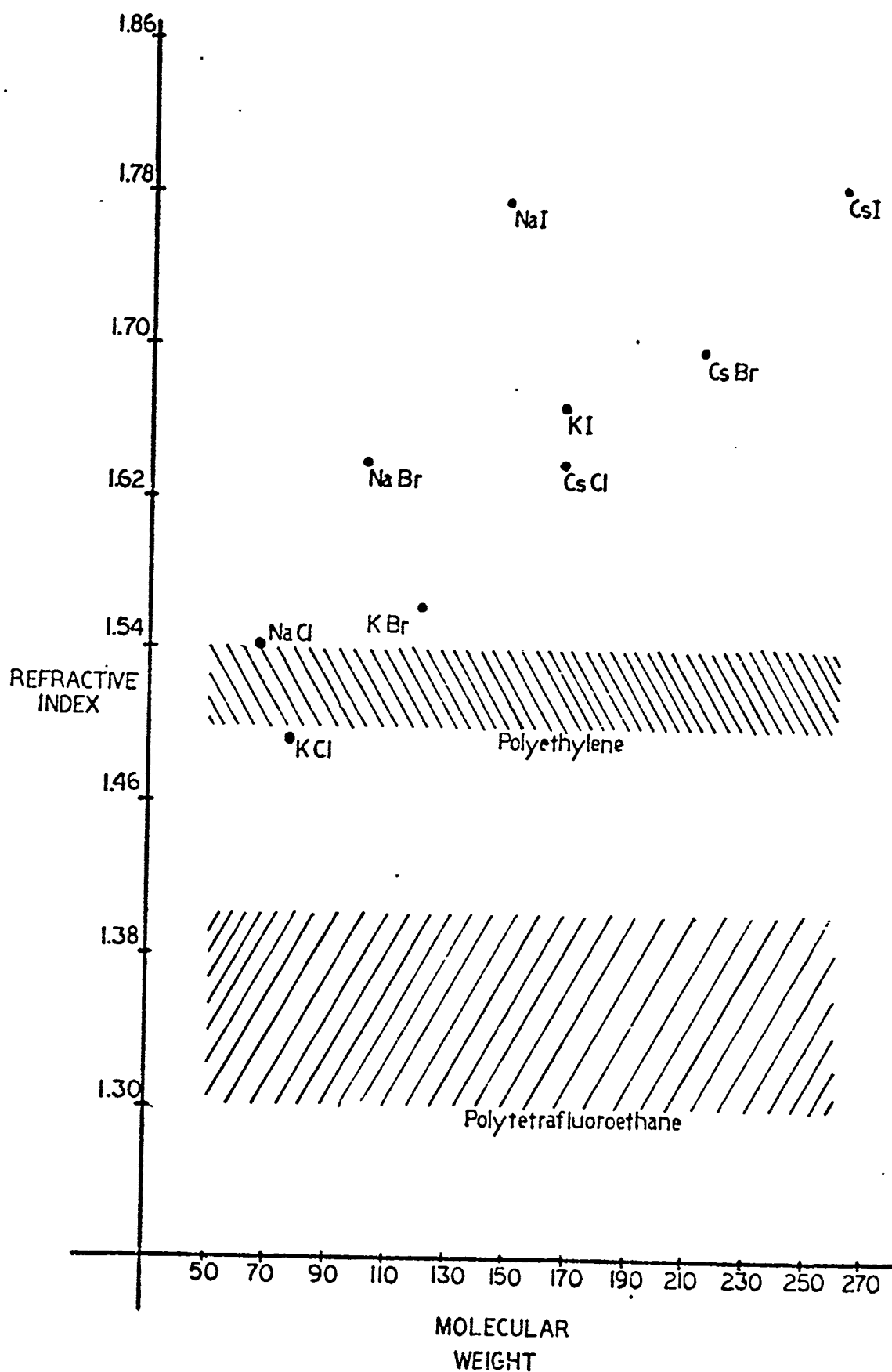


Fig. 18. Index of refraction vs. formula weight for the alkali halides.

screen and dipped several times into the polyethylene solution. Scanning electron micrographs showed the coatings were discontinuous and water resistance was poor. The lack of uniform coverage could have been due to the relatively low concentration of polyethylene in saturated p-xylene (~2 wt.%). A second method involved evaporating to dryness at 135°C a quantity of KCl crystallites immersed in a small amount of polyethylene saturated p-xylene. The solution was stirred continuously during evaporation to promote a more even coating on the KCl crystallites. Scanning electron micrographs showed a more even coating than in the previous case. A third experiment involved an attempt to coat KCl crystallites directly with molten polyethylene. The attempt was unsuccessful due to the high viscosity of molten polyethylene which prevented any sort of uniform coating being achieved.

Windows were pressed under vacuum from coated KCl crystallites using a standard Perkin-Elmer KBr die. Forces of 20,000 pounds and temperatures of 25°C and 110°C were used to form translucent discs 13 mm in diameter and 1 mm thick. A Perkin-Elmer LR10 infrared spectrometer was used to test window transmittance from 7.5 to 20 μ m. Degradation of infrared transmittance was determined by taking spectra before and after the discs were immersed in water for constant lengths of time. Figure 19 shows the results of these experiments for 1 mm thick windows prepared by several techniques. The data show that for both hot pressed and cold pressed composite windows an almost immediate increase in absorbance occurs on exposure to water. Furthermore, after only two minutes exposure there is nearly a 100% increase in absorbance. The decrease in absorbance of the uncoated KCl window is attributed to the decrease in thickness brought about by dissolution. Figure 20 shows a scanning electron micrograph (SEM) of an uncoated KCl crystallite at 500X; Figure 21 is a similar micrograph of a polyethylene coated crystallite prepared by the solvent evaporation technique. The discontinuous nature of the coverage by the coating is readily apparent in the micrograph. Figure 22 is a micrograph of an uncoated KCl crystallite at 5,000X. Figure 23 is a micrograph at 5,000X of a coated crystallite; here the nonuniformity in the coating is shown even more clearly than in Figure 21. Figure 24 shows a portion of an uncoated window at 500X after water treatment; a portion of a coated window after similar exposure is shown in Figure 25, also at 500X.

It is obvious that polyethylene presents considerable difficulties in obtaining a uniform, continuous, fully water-resistant coating. A possible explanation for this lies in polyethylene's relatively simple structure (for a polymer) which favors crystallization from solution in discontinuous platelets or lamellae. Further work might be directed toward

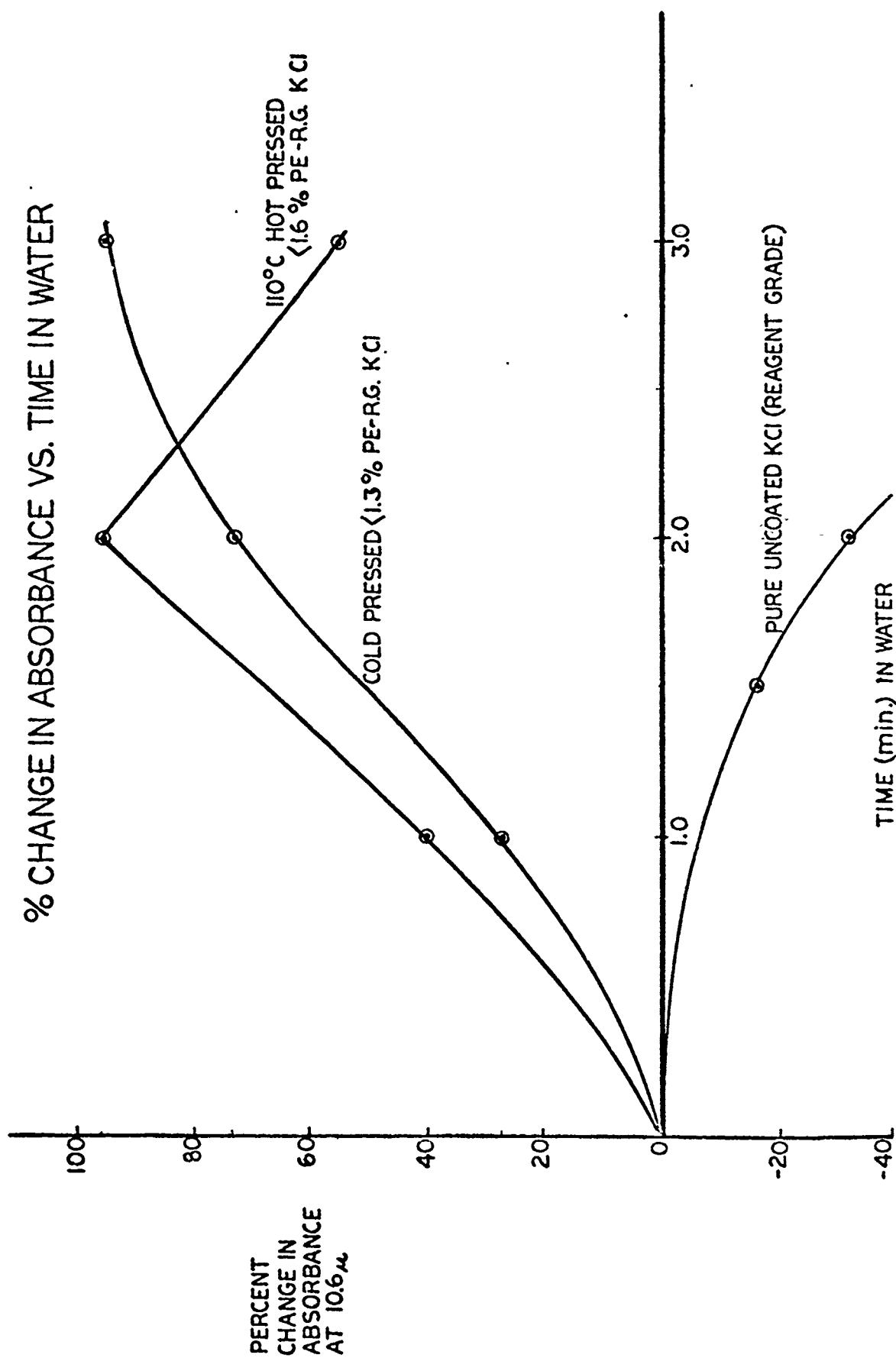


Fig. 19. Change in absorbance of treated KCl as a function of water exposure.

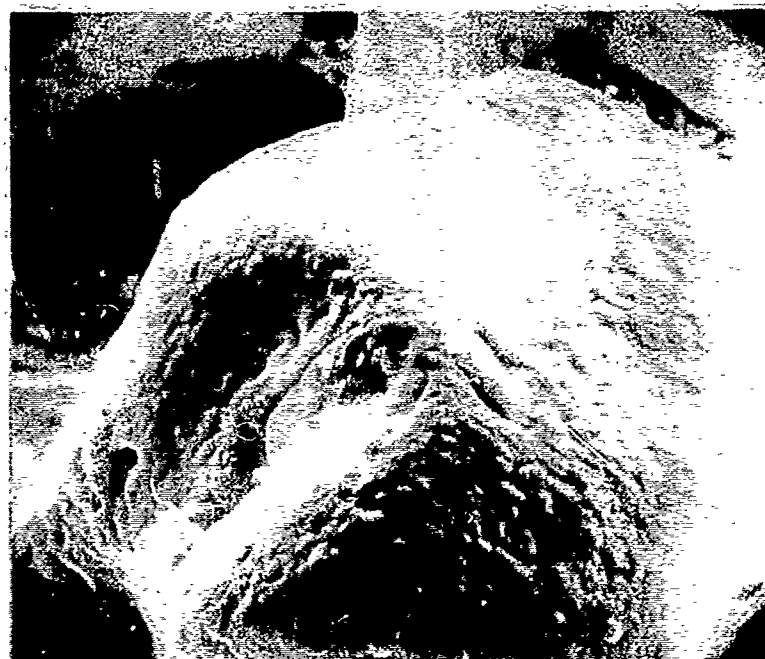


Fig. 20. SEM of uncoated KCl at 500X.

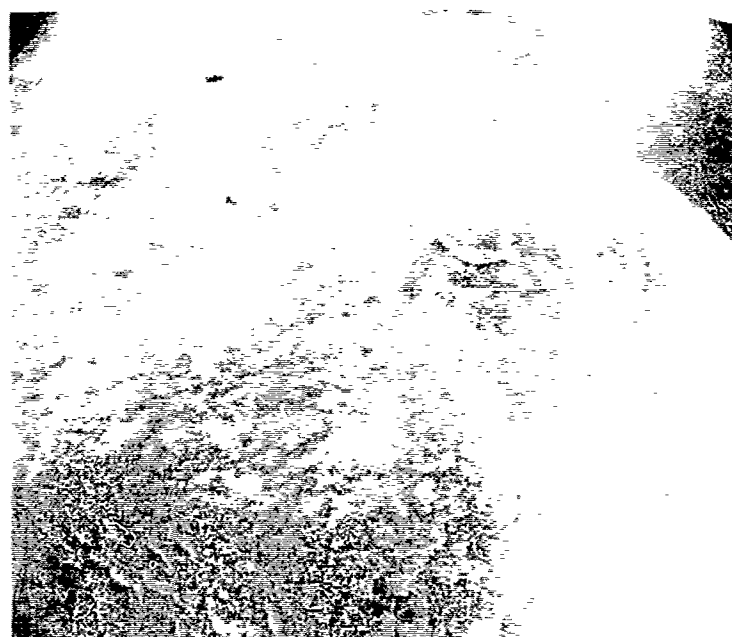


Fig. 21. SEM of polyethylene-coated KCl at 500X.

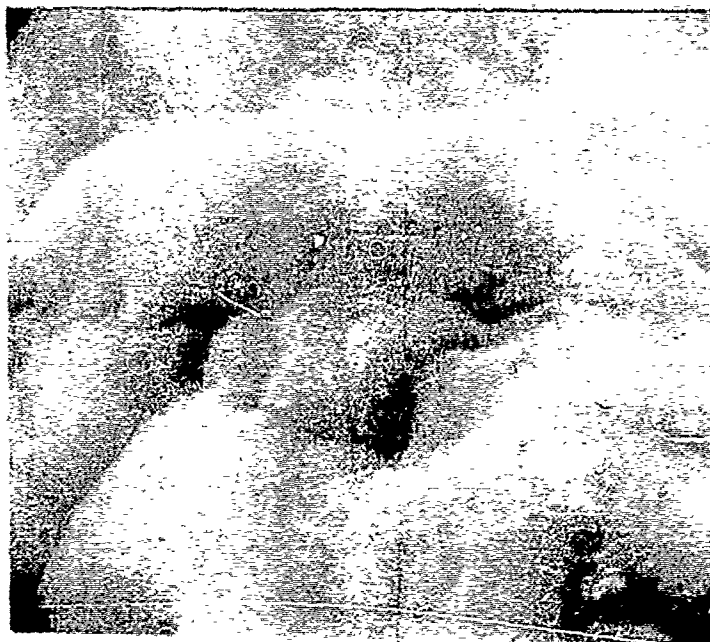


Fig. 12. SEM of uncoated KCl at 5,000X.

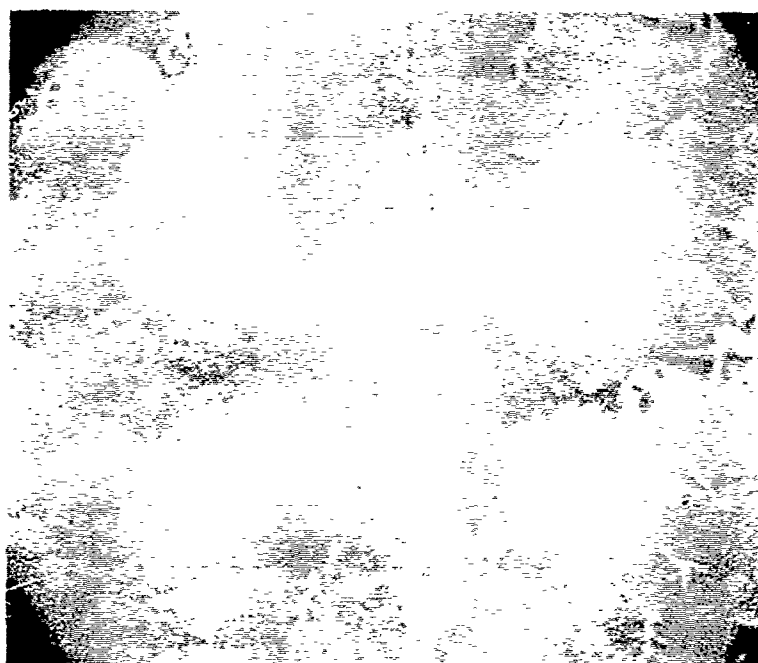


Fig. 13. SEM of polyethylene coated KCl at 5,000X.

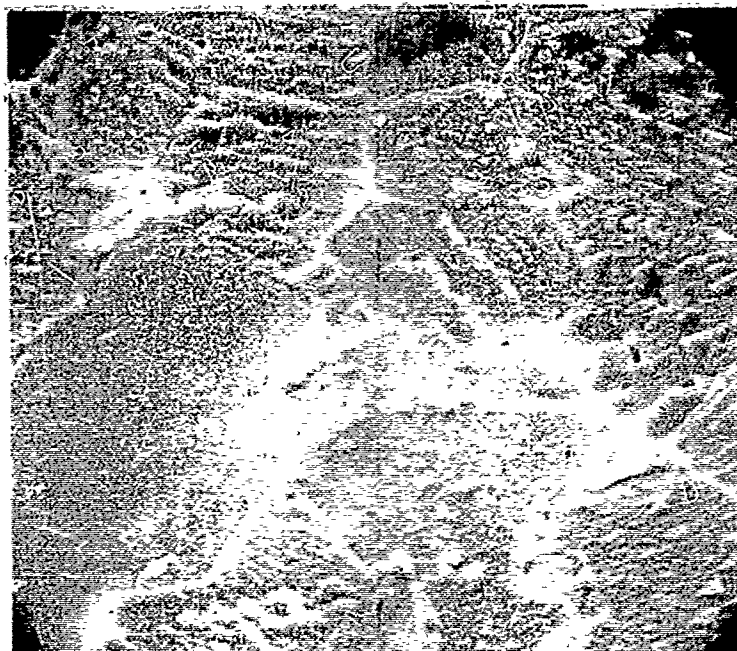


Fig. 14. SEM of uncoated KCl window after water treatment.



Fig. 15. SEM of polyethylene coated KCl window after water treatment.

testing other coatings which have more suitable properties, among which are polypropylene, polystyrene and tetraphenyl borate (a compound which has a strong attraction for the alkali halides). So far, however, attempts to produce a water-resistant alkali organic composite have not been successful. The concept, however, offers high potential for a tough environmentally protected window but requires a more extensive study of the chemistry of the inorganic-organic interface than can be carried out under the present program.

C. Chalcogenide Coatings

As a result of the problems mentioned above, studies on chalcogenide coatings were initiated. Unfortunately, expiration of the contract prevented the accumulation of more than a very limited quantity of data. $\text{Ge}_3\text{Se}_5\text{As}$ and $\text{GeSe}_{1.25}$ were chosen for the preliminary experiments because of their good infrared transmission and ease of deposition by flash evaporation. The fact that the chalcogenides have a significantly higher index of refraction than the alkali halides was not considered of crucial importance because of the possibility of reducing reflectance losses by an appropriate multilayer coating (see Appendix B for a simple analysis of this problem). In order to minimize the number of experimental variables affecting the results, the intergranular coating approach was not used in the first studies; surface coatings only were prepared.

The substrates were pellets of optical grade KBr prepared in the same way as in the case of the polymer coated samples. $\text{Ge}_3\text{Se}_5\text{As}$ or $\text{GeSe}_{1.25}$ was flash evaporated onto the substrate in a Veeco vacuum system maintained in the neighborhood of 10^{-6} torr. Pellets were coated as quickly after preparation as possible to minimize any surface contamination. The coating thicknesses produced were on the order of 1,000 Å.

Water exposure tests were designed to study the adhesion of the coating to the KBr substrate as well as its permeability to moisture under fairly severe conditions. This was done by allowing a specific quantity of water to fall from a buret onto the surface of the sample from a set height; the force of the water striking the coated surface could be varied by varying the height of the buret. Initial conditions were a buret to sample distance of 5 cm and flow of 22 ml/min.

The time available for the experiments was not sufficient to optimize the coating procedure. Figure 26 is an optical micrograph of an as-prepared $\text{Ge}_3\text{Se}_5\text{As}$ coated KBr pellet; as can be seen, there are numerous scratches on the surface. It was not determined whether the scratches were present before coating or resulted from improper handling techniques, but their presence undoubtedly affects the samples water resistance.

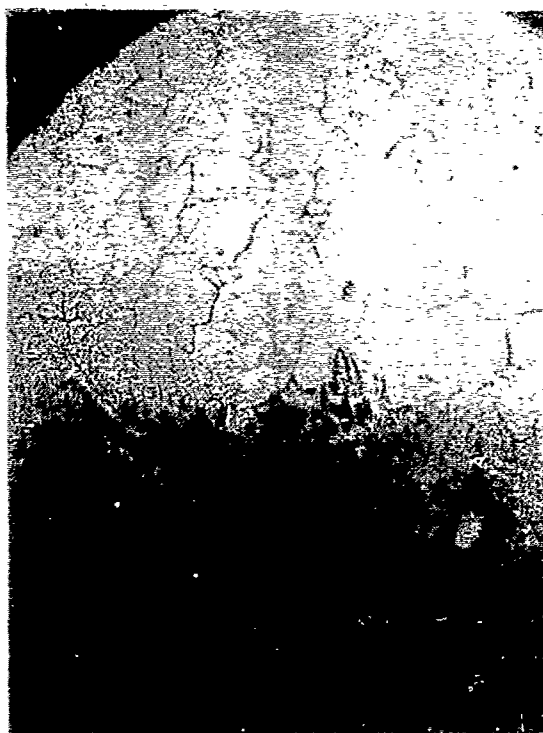


Fig. 26. $\text{Ge}_7\text{Se}_5\text{As}$ coated KBr, untested surface. 200X.



Fig. 27. $\text{Ge}_7\text{Se}_5\text{As}$ coated KBr, after water tested. note coating is cracked.



Results of the water tests differed for the two coating materials. The $\text{Ge}_3\text{Se}_5\text{As}$ was very quickly removed by the falling water stream. The force of the water seemed to undermine the coating, causing it to wrinkle and peel off. However, the coating itself appeared to remain intact and was otherwise unaffected by the water treatment (see Figure 27). It is hypothesized that defects in the coating allowed water to penetrate and dissolve the substrate, floating off the coating. Experiments to prepare very high quality coatings by flash evaporating on vacuum-cleaved single crystals could not be complete before the termination of the contract.

The results of water tests on $\text{GeSe}_{1.25}$ coated KBr pellets produced different results. Water protection was not significantly improved over the $\text{Ge}_3\text{Se}_5\text{As}$ coating, but deterioration resulted from penetration of water through the coating. The coating seemed to adhere better to the substrate, but to be more porous to water. See Figure 28.

Although neither coating imparted any degree of water protection to the KBr substrate, the fact that the failure mechanism appeared to be so different in the two cases gives hope that further work might produce a truly protective coating. For example, a layered coating with $\text{GeSe}_{1.25}$ next to the substrate and $\text{Ge}_3\text{Se}_5\text{As}$ on top of it might provide the combination of adherence and resistance to water penetration required for a good coating. The very preliminary experiments reported here can only suggest that more work in the area would be profitable.

X. Conclusion

It must be concluded that more work is needed to capitalize fully on the advances made in the twelve months covered by this report. As stated in the introduction, our principle objectives were two-fold: (1) to evaluate the limitations of glasses as high powered laser windows and (2) to attempt to produce a strengthened, water resistant, alkali-halide based polycrystalline compact through a novel intergranular coating approach. Rather than concentrate on a single, narrow area, our intent was to conduct a research survey of a wide variety of unorthodox approaches to problems attendant to the design of a high power laser window. Significant progress toward meeting these objectives has been made. Work was done in all nine of the research sub-categories listed in the Introduction; some questions have been answered and problem areas for further research have been identified.

In particular the following results were obtained:

Chalcogenide Glasses

- (1) Homogeneity limits for the chalcogenide glasses studied

were determined. The thin film materials are homogenous at least down to a scale of 100 Å. Phase separation was not found in the bulk glasses studied here.

- (2) The chalcogenide glasses in the Ge-Se-As and Ge-Se-Sb systems reported here are extremely stable toward thermally induced structural changes, at least up to temperatures on the order of the glass transition.
- (3) The most probable contributions to high infrared absorption at 10.6μm are the presence of microvoids or Ge-O bonds. The absorption seen with the samples studied by us was not due to impurities present in either the Se or As used in their fabrication.
- (4) The infrared absorption at 10.6μm was significantly lowered by internal gettering as the result of addition of 0.15 to 0.36% Ti. Addition of Zr did not result in lowered infrared absorption.
- (5) The mechanical behavior of Ge-Se-As and Ge-Se-Sb glasses was investigated as a function of heat treatment. Microhardness of both glasses was unaffected by heat treatment while the modulus of rupture is slightly decreased. Similarly, the bulk tensile strength of the Ge-Se-As glass shows a small decrease with extensive thermal treatment.

Coated Alkali Halides

A novel, intergranular coating technique was used in an attempt to fabricate a water resistant window, but it met with only limited success. Windows were fabricated, but water resistance was unsatisfactory. The use of organic polymers for coatings shows promise, but real progress requires detailed surface studies which are beyond the scope of the research reported here. Limited tests with chalcogenide coatings give some cause for optimism that an intergranular chalcogenide coating technique for polycrystalline alkali halides windows could be successful.

XI. References

1. C. S. Sahagian and C. A. Pitha, eds., Conference on High Power Infrared Laser Window Materials, AFCRL-71-0592.
2. D. G. Thomas "Ceramics and Glasses: Some Uses in the Communications Industries" in Physics of Electronic Ceramics, Part B, L. L. Hench and D. B. Dove, eds., Marcel Dekker, New York, 1971. pp1057.
3. See for example the series of papers by A. R. Hilton J. Non-Crystalline Solids 2, 28 (1970).
4. A. R. Hilton, C. E. Jones and M. Brau, Phys. Chem. Glasses, 7 [4], 105 (1966).
5. D. B. Dove, M. B. Heritage, K. L. Chopra and S. K. Bahl, Appl. Phys. Letters, 16, 138 (1970).
6. H. L. Luo, M. S. Thesis, California Institute of Technology, 1964; A. Bienenstock, F. Betts and S. R. Ovshinsky, J. Non-Crystalline Solids, 2, 347 (1970); F. Betts, A. Bienenstock and S. R. Ovshinsky, J. Non-Crystalline Solids, 4, 554 (1970).
7. W. C. Lacourse and V. A. Twaddell, J. Non-Crystalline Solids, 3, 234-236 (1970).
8. "Structure, Properties and Radiation Sensitivity of Electrically Bistable Materials," AROD Contract ARPA DAHCO4-70-C-0024.
9. B. E. Warren, X-Ray Diffraction, Addison-Wesley Publ., Reading, Mass., 1969.
10. C. W. B. Grigson, Rev. Sci. Instr., 36, 1587 (1965); D. B. Dove and P. N. Denbigh, Rev Sci. Instr., 37, 1687 (1966).
11. T. Takemori, R. Roy and G. J. McCarthy, Matls. Res. Bull., 5, 592 (1970).
12. B. J. Molnar, "Structure of Amorphous Ge-Se Films" M. S. Thesis; University of Florida, (1971).
13. A. R. Hilton and C. E. Jones, Phys. Chem. Glasses, 7, 114 (1966).

14. D. Lezal and I. Srb, Collection Czechoslov. Chem. Commun., 36, 2091-2092 (1971).
15. L. L. Hench, D. B. Dove, R. E. Loehman, "Thermal History Effects on the Structure and IR Transmission of Laser Window Glasses", Conference on High Power Laser Windows, pp 131, AFCRL-71-0592, Special Report #127.
16. W. C. Lacourse, "The Strength of Glass" in Introduction to Glass Science, L. D. Pye., H. J. Stevens, W. C. Lacourse, eds., M. Delsher Inc. Publisher, 1972, pp 451.
17. A Rudnick, A. R. Hunter, F. C. Holden, Maten. Res. Stand. 3 [4] 283-89 (1963).
18. A. R. Hilton, Appl. Optics 5, No. 12 (1966) pp 1877.
19. A. R. Hilton, J. Non-Cryst. Solids. (1970) 28-39.
20. A. R. Hilton, D. E. Jones, M. Brau , Phys. & Chem. of Glasses, Vol. 7, No. 4 (1966) pp 108.
21. F. A. Horrigan and T. F. Deutsch, "Materials and Structures for High Powered Lasers," presented at the High Power Infrared Laser Window Materials Conference, Boston, Mass., October 27, 1971.
22. W. Kingery, Introduction to Ceramics, John Wiley, New York, 1960
23. A. A. Griffith, Phil. Trans. Royal Soc. (London), A221, 163 (1920).
24. S. M. Wiederhorn, "Fracture of Ceramics," in Mechanical and Thermal Properties of Ceramics, J. B. Wachtman, Jr., ed., NBS Special Publ. 303, 1969, pp. 217-241.
25. R. M. Fulrath and J. A. Pask, eds., Ceramic Microstructures, John Wiley, New York, 1968, p. 379ff.

Appendix A

12. Thermal History Effects on the Structure and IR Transmission of Laser Window Glasses

L.L. Hench, D.B. Dove and R.E. Loehman
University of Florida
Gainesville, Florida 32601

Abstract

Thermal effects in glasses are discussed, drawing on experience with radial distribution analysis, electron microscopy and other techniques obtained with several glass systems. The relevance of these observations, to effects likely to occur during thermal exposure of infrared laser windows is commented upon. A recent advance in analysis of the thermal-stress-atmosphere dependent changes in glasses is reviewed and related to laser window applications.

1. INTRODUCTION

Many properties of glasses are dependent not only upon composition but also upon material thermal history. Both local atomic configurations and material microstructure may be altered by exposure to high temperatures, while structural alterations in turn give rise to changes in physical properties. Because of energy absorption during transmission of the laser beam, the properties of a window material may undergo both reversible and irreversible changes depending on the temperature and time of exposure. Thermal effects may be classified as reversible effects leading to undesirable change in optical characteristics and as irreversible effects leading to window aging and ultimately failure. Two possible applications of prior thermal treatments may be noted, firstly in the stabilization of properties to minimize aging, and secondly, the possibility exists that prior heat treatment, using the transmitted beam itself, may be

employed to induce irreversible changes that cancel the reversible changes, making a window that is good optically when operating at a chosen transmitted beam power. Finally, environmental thermal effects such as ambient gas diffusion and surface degradation must be considered. The objectives of this paper are to discuss thermal effects in glasses generally, and to present some preliminary results on thermal history effects in infrared transmitting glasses within the Ge-Se-Se system.

2. THERMAL HISTORY EFFECTS ON GLASS ULTRASTRUCTURE

In this discussion the term ultrastructure designates the atomic or ionic configurations which exist in a glass within a distance of order 10 \AA about any reference atom or ion. Such localized structures are determined on a statistical basis by electron, x-ray or neutron diffraction techniques. Several studies [Tatarinova (1959), Hilton *et al.* (1966), Bienenstock *et al.* (1969), Dove *et al.* (1970), Mikolaichuk and Dacheck (1971)] have applied diffraction techniques to the analysis of the ultrastructure of chalcogenide glasses. In one of the more recent studies, from this laboratory [Molnar (1971), Dove, Molnar and Chang (1971)], the intensity profiles across the electron diffraction patterns of thin films of $\text{GeSe}_{0.7}$ and $\text{GeSe}_{2.4}$ glasses were determined using direct electronic recording with electrostatic rejection of inelastically scattered electrons. Radial distribution analysis of the $\text{GeSe}_{0.7}$ (and also of GeSe) intensity curves indicates that the local atomic order in these films differs from the local order to be expected for the distorted rock salt structure of crystalline GeSe . In addition, films of composition $\text{GeSe}_{2.4}$ did not possess a local order corresponding to the crystalline, distorted CdI layer structure of GeSe_2 . The bonding characteristics of these glasses is therefore expected to be considerably different from that of either of the two mentioned crystalline phases.

The films were found to be susceptible to both thermal treatment and to exposure to the electron beam with considerable changes occurring in the diffuse diffracted intensity prior to the evident formation of microcrystalline regions of selenium. Radial distribution analysis of these intensity curves showed changes in nearest neighbor coordination as in Fig. 1. It can be noted that the area

under the peak increases and a new peak appears at 2.90 \AA . These change can be interpreted as due to structural rearrangements associated with the development of GeSe and other phases. It is significant to note that the above changes occur prior to the observation of crystallization by electron microscopy. Conversely it has also been found that the absence of crystalline peaks in a diffraction pattern from a glassy material does not rule out the presence of a small volume fraction of microcrystallites. Electron microscopy on these glassy films showed a homogeneous microstructure at least down to a scale of order 20 \AA . Diphasic structures, however, have been observed in a certain chalcogenide compositions [Takemori *et al.* (1970)]. Recent x-ray analysis of local order in an oxide glass SiO_2 using pair function distribution techniques has followed thermal effects out as far as the fifth coordination shell [Gokularathnam *et al.* (1971)].

Thermally induced changes in the nearest neighbor atomic configurations imply that the infrared absorption of these glasses may be significantly affected by thermal exposure. Consequently, the possibility exists of modifying regions of the infrared transmission spectrum by heat treatment. Changes in bonding may also give rise to changes in the refractive index and its thermal coefficient which, although small, may yet be significant for the present application. A major aim in material selection and treatment is to minimize reversible thermal effects and, if possible, to avoid irreversible effects altogether.

Schematically, irreversible changes in laser window properties with time at constant temperature are shown to arbitrary scale in Fig. 2. Longer time exposures which induce crystallization will be discussed in the following section. If structural changes are brought about in the window by the beam generated temperature profile, then an irreversible gradient in properties will be created. This effect is illustrated in Fig. 3, where it is shown how reversible and irreversible effects may combine additively or alternatively in opposition to reduce thermal effects. A change in properties, of course, in turn may modify the temperature distribution. Clearly it is necessary to select a glass which does not undergo ultrastructural changes at the temperatures and time periods reached during operation. The effects of reversible thermal effects must also be

minimized by materials choice and treatment. A study of thermal treatment of glasses is therefore necessary to provide information on window life, aging characteristics, and may possibly lead to a useful means of property modification.

3. THERMAL EFFECTS ON GLASS MICROSTRUCTURE

Thermal treatment of glasses can result in crystallization which may affect optical properties and significantly influence laser window behavior. Key properties such as yield strength, thermal expansion coefficient, softening point and optical absorption may change in a manner dependent on the volume fraction V_v of second phase generated and therefore are both time and temperature dependent. As noted in Fig. 3, irreversible changes may possibly be used to control material properties advantageously; however, it is not known to what (small) extent a glassy or other phase separation may proceed before light scattering becomes significant.

Recent results from this laboratory have documented a number of property changes in oxide glasses. Microstructural dependent changes in softening point, thermal expansion coefficient, elastic modulus and fracture strength of $\text{Li}_2\text{O-SiO}_2$ glasses are shown in Figs. 4, 5, 6 and 7, respectively.

4. STRUCTURAL MODELS FOR CHALCOGENIDE GLASSES

It is informative to consider atomic structural models for the chalcogenide glasses. Radial distribution analysis yields a value for the distance between nearest neighboring atoms and provides a measure of the nearest neighbor coordination number averaged over all atoms. The results for the germanium chalcogenides are in most cases consistent with each germanium atom having four neighbors and each selenium atom having two, with effective atomic radii lying close to the covalent radii values. One model for a binary glass, for example, $\text{Ge}_x\text{Se}_{1-x}$, is that of a three-dimensional (primarily) covalently bonded structure in which bonds between the two types of atoms are distributed randomly. As pointed out by Fawcett, Wagner and Cargill (1971), the numbers of Ge-Ge, Se-Se and Ge-Se bonds in

such a case are respectively $4x^2N/(1+x)$, $(1-x)^2N/(1+x)$, $4x(1-x)N/(1+x)$. It is readily verified that the total number of bonds of any type is $(1+x)N$ where N is the total number of atoms. With the assumption that system energy is largely due to the strong bonding between nearest neighbor, the heat of mixing of the glass (relative to the solid elemental constituents) may be estimated,

$$\frac{\Delta H}{N} = \frac{x(1-x)4\delta}{1+x}$$

using the approximate expression relating bond energies given by Pauling (1960).

$$H_{AB} = \frac{1}{2}(H_{AA} + H_{BB}) + \delta$$

where $\delta = 23|\epsilon_A - \epsilon_B|^2$; ϵ_A and ϵ_B are the Pauling electronegativities of elements A and B, and H_{AA} , H_{BB} , H_{AB} are the bond energies for bonds between atoms of type A-A, B-B and A-B. This is a simplistic approach but does allow some interesting comparisons to be made. The result for $\text{Ge}_x\text{Se}_{1-x}$ is

$$\frac{\Delta H}{N} = 33 \frac{x(1-x)}{1+x} \text{ kcal/gmol}$$

A much higher value is obtained if an ordered structure is assumed, that is, one in which Ge and Se atoms alternate as far as possible throughout the glassy network. At the composition GeSe_2 this is just the analogue of the vitreous silica structure, with every Ge surrounded by four Se atoms and every Se surrounded by two Ge atoms. The numbers of Ge-Ge, Se-Se and Ge-Se bonds are respectively 0, $4xN$, $(1-3x)N$ for $0 \leq x \leq 1/3$ and $(3x-1)N$, $2(1-x)N$, 0 for $1/3 \leq x \leq 1$. The heat of mixing then becomes

$$\frac{\Delta H}{N} = 33x \text{ kcal/gmol} \quad 0 \leq x \leq 1/3$$

and

$$\frac{\Delta H}{N} = 17(1-x) \text{ kcal/gmol} \quad 1/3 \leq x \leq 1$$

Using the very approximate estimates outlined above, the ordered arrangement is at least energetically preferred near the GeSe_2 composition (entropy contributions being neglected). In GeTe_2 a similar estimate suggests that the ordered structure is less strongly preferred and, when configurational entropy is considered, the random bonding model may be preferred even at moderate temperatures. Evidently the elucidation of a valid structural model is of significance for a discussion of infrared absorption, thermal stability and other properties. Work in this laboratory has been directed toward obtaining free energy curves for the germanium chalcogenides from quasi-chemical considerations. Qualitatively the occurrence of the eutectic in the Ge-Te phase diagram is associated with the absence of a GeTe_2 phase in the equilibrium diagram. The free energy curve of the liquid phase then touches the tangent line between crystalline Te and GeTe at an intermediate composition when the temperature is raised. In the Ge-Se system, the eutectic is suppressed by the existence of a GeSe_2 phase. In this case the liquid free energy curve intersects the tangent line between Se and GeSe_2 at the selenium end instead of at an intermediate composition. It is hoped that the present calculations may be applied to the ternary case in order to provide insight into the bonding characteristics and ordering tendencies as composition and temperature are varied.

Figure 8 illustrates some of the changes in infrared transmission behavior that can occur in chalcogenide glasses as a result of heat treatment and compositional variation. The upper curves show a small increase in infrared transmission for 2.5 mm thick slices of $\text{Ge}_2\text{Se}_3\text{As}$ as a function of surface polishing. These curves remained unchanged after heat treatments of up to 9-1/2 hours at 327°C . The lower curves, however, show an increase in IR transmittance for $\text{Ge}_{33}\text{Se}_{55}\text{As}_{12}$ as a result of heat treatment. In neither composition did the heat treatments mentioned bring about detectable crystallization. It should be noted that the region of high transmittance beginning at $8\text{ }\mu\text{m}$ for $\text{Ge}_2\text{Se}_3\text{As}$ is considerably broader than the corresponding region in $\text{Ge}_{33}\text{Se}_{55}\text{As}_{12}$. The two compositions basically are GeSe_4 with differing amounts of As substituted for Se; here a small increase in As greatly broadens the transmission region.

5. ENVIRONMENTAL AND STRESS EFFECTS ON LASER WINDOWS

Stress enhanced surface corrosion is an effect which may also be of importance to the stability of laser windows. Atmospheric dependent strength deterioration of glasses and ceramics has been known for many years [Charles (1958)]. Recent results from this laboratory [Sanders *et al.* (1971)] using infrared reflection spectroscopy and atomic emission spectroscopy have shown that a reaction occurs on the surface of glass exposed to water vapor; this surface reaction shifts the infrared absorption spectrum significantly. It has also been found that applied stresses increase the rate of surface reaction, while temperature excursions of only 25 to 75°C above ambient increased reaction rates by 3 to 4 orders of magnitude.

These observations suggest that conditions at the surface of a window may give rise to stress-atmospheric corrosion attack, due to stresses and temperatures induced by the beam.

6. SUMMARY

Thermal effects upon glassy materials have been discussed with reference to laser window design, and the possibility of using heat treatment to stabilize or to modify properties is noted. Previous measurements on chalcogenide glasses have indicated the occurrence of ultrastructural changes occurring prior to temperature induced phase separation. Present work is directed to the thermal stability of Ge-Sc-Se glasses and some preliminary results have been introduced.

REFERENCES

- Betts, F., Bienenstock, A., and Ovshinsky, S. R., J. Non-Cryst. Solids, 4, 554-63 (1979).
- Charles, R. J., J. Appl. Phys., 11, 1549 (1958).
- Dove, D. B., Heritage, M. B., Chopra, K. L., and Bahl, S. K., Appl. Phys. Letters, 16 (1970).

- Dove, D. B., Molnar, B., and Chang, J., 4th Int. Conf. on Amorphous Semiconductors, to appear.
- Fawcett, W., and Cargill, 4th Int. Conf. on Amorphous Semiconductors, to appear.
- Gokularathnam, C. V., Gould, R. W., and Hench, L. L., American Ceramic Society Special Publication, "Nucleation and Crystallization Revisited," 1971.
- Mikolaichuk, A. G., and Kogut, A. N., Sov. Phys. Cryst., 15, 296 (1970); Hilton, A. R., Jones, C. E., Dobrott, R. D., Klein, H. M., Bryant, A. M., and George, T. D., Phys. Chem. Glasses, 4, 116 (1966).
- Molnar, B., Masters Thesis, University of Florida, 1971.
- Pauling, L., in The Nature of the Chemical Bond, Cornell Press, 1960.
- Sanders, D. M., Person, W. D., and Hench, L. L., Applied Spectroscopy (submitted to).
- Takemori, T., Roy, R., and McCarthy, G. J., Mat. Res. Bull., 5, 529 (1970).
- Tatarinova, L. I., Sov. Phys. Cryst., 4, 637 (1959).

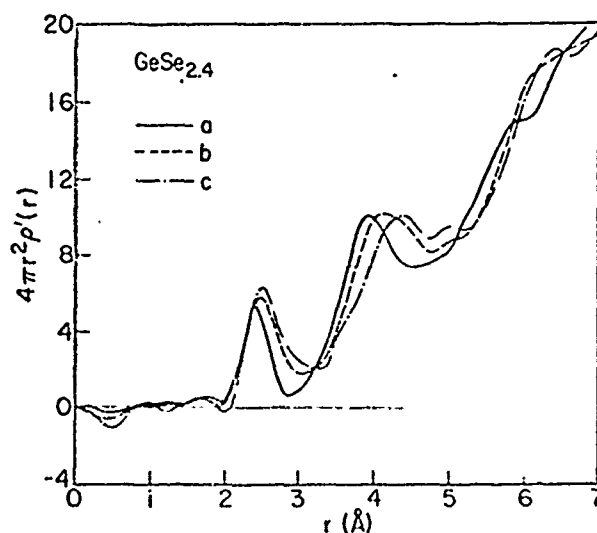


Figure 1. Radial Distribution Function of $\text{GeSe}_{2.4}$. Curve a - as deposited. Curves b and c - after progressive amounts of heat treatment

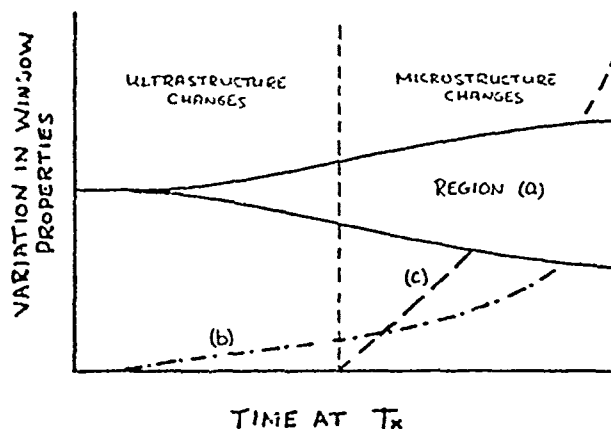


Figure 2. Irreversible Time Dependent Changes Accompanying Ultrastructural and Microstructural Alterations in a Laser Window Material at Temperature T_x . Region (a) - region of variation of fracture strength, softening or melting point, thermal conductivity, index of refraction and percent absorption. Region (b) - relative change in ultrastructure. Region (c) - V_v , the volume fraction of crystallites formed

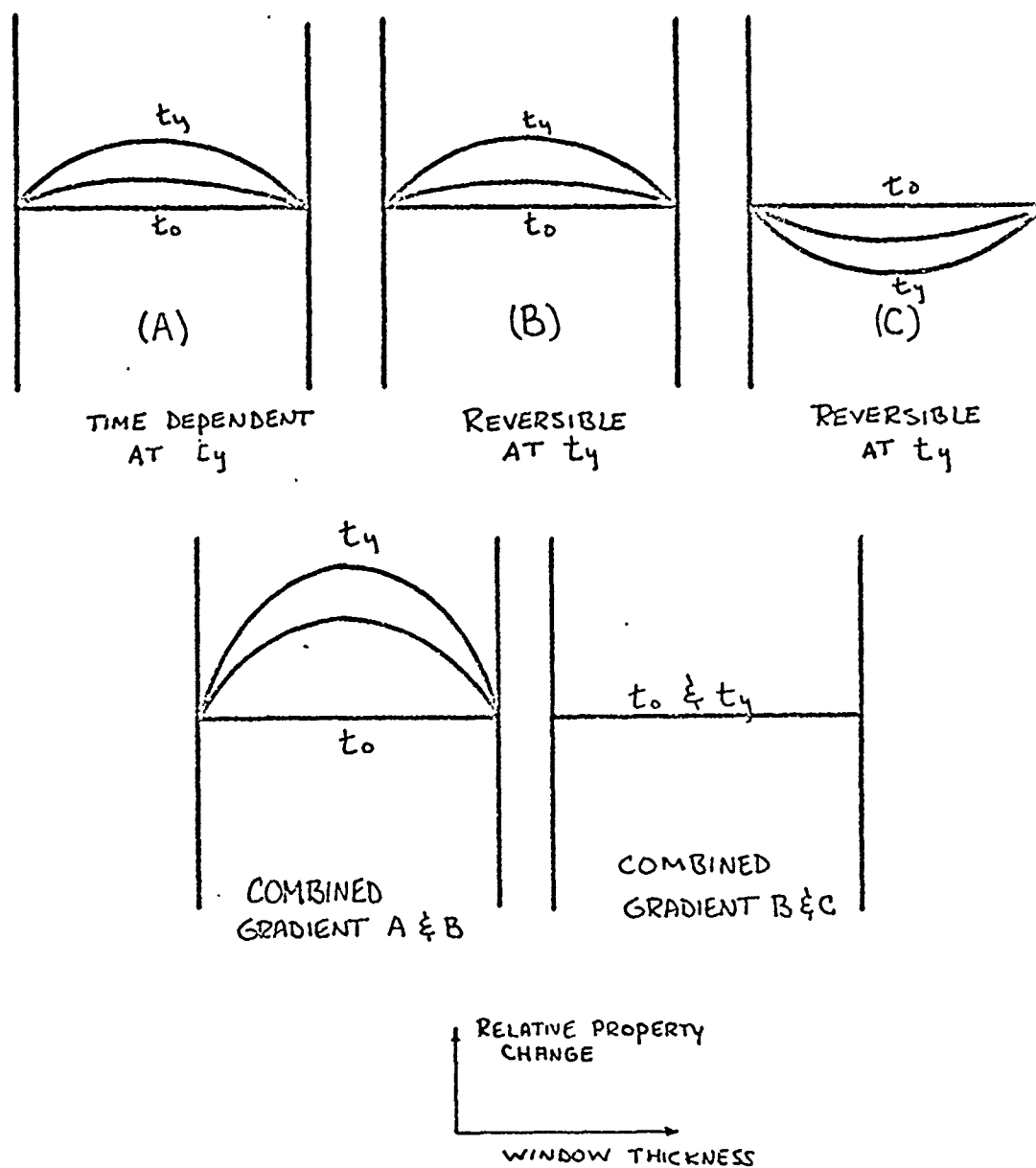


Figure 3. Amplitude of Property Gradients Due to Time Dependent Structural Changes as a Function of Sample Thickness

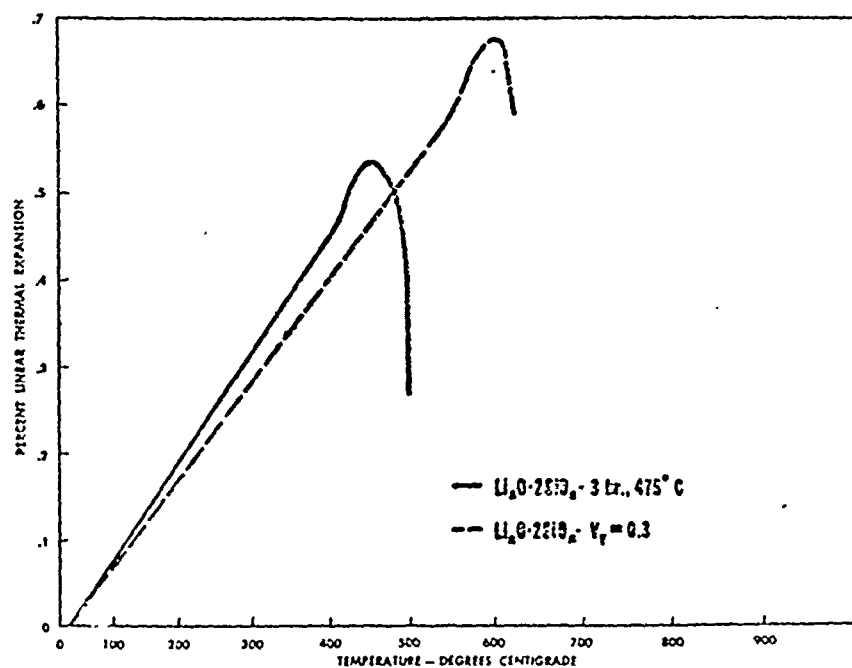


Figure 4. Percent Linear Thermal Expansion of $\text{Li}_2\text{O}-\text{SiO}_2$ Glasses as a Function of Volume Fraction of Crystallites

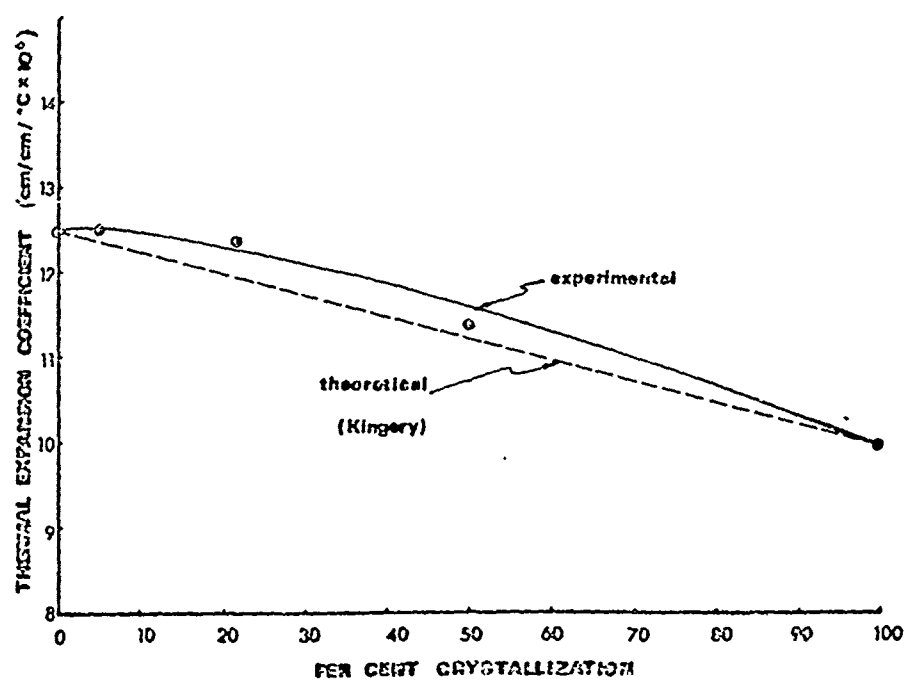


Figure 5. Thermal Expansion Coefficient of $\text{Li}_2\text{O}-\text{SiO}_2$ Glasses as a Function of Volume Fraction of Crystallites

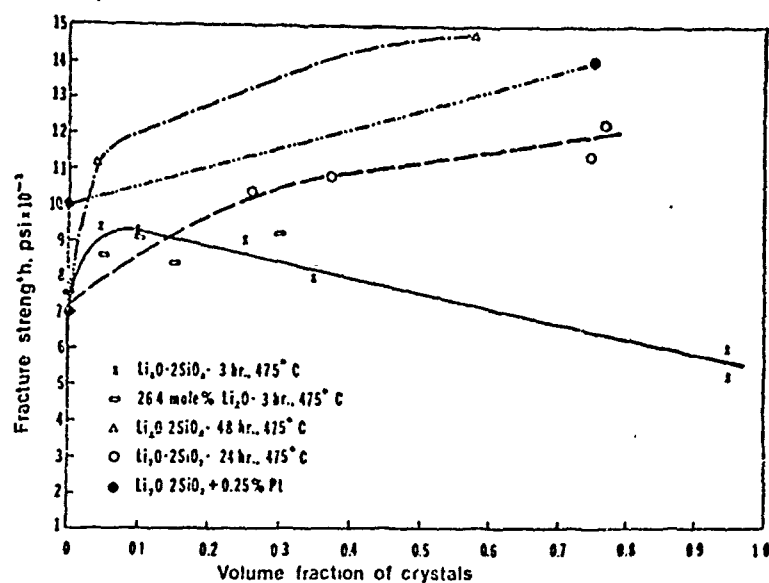


Figure 6. Fracture Strength of $\text{Li}_2\text{O} \cdot \text{SiO}_2$ Glasses as a Function of Volume Fraction of Crystallites

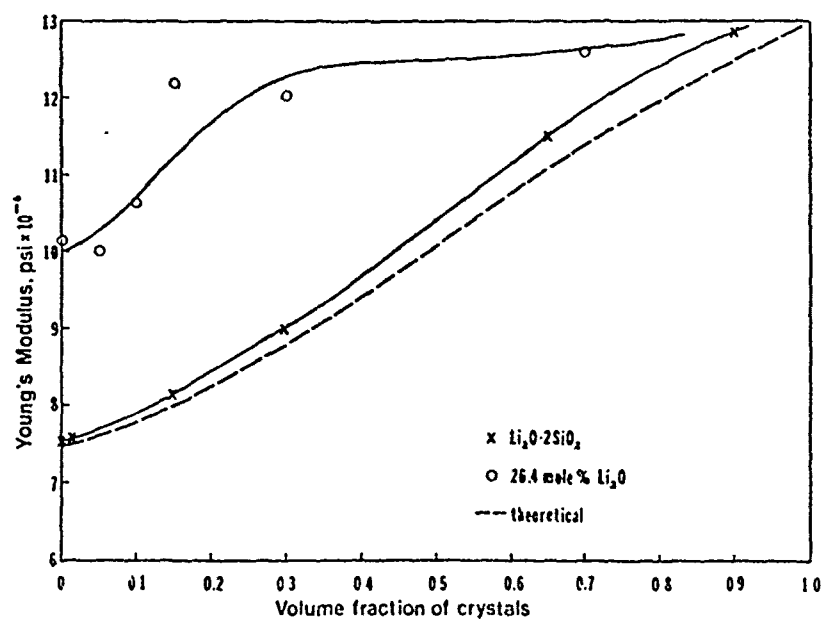


Figure 7. Young's Modulus of $\text{Li}_2\text{O} \cdot \text{SiO}_2$ Glasses as a Function of Volume Fraction of Crystallites

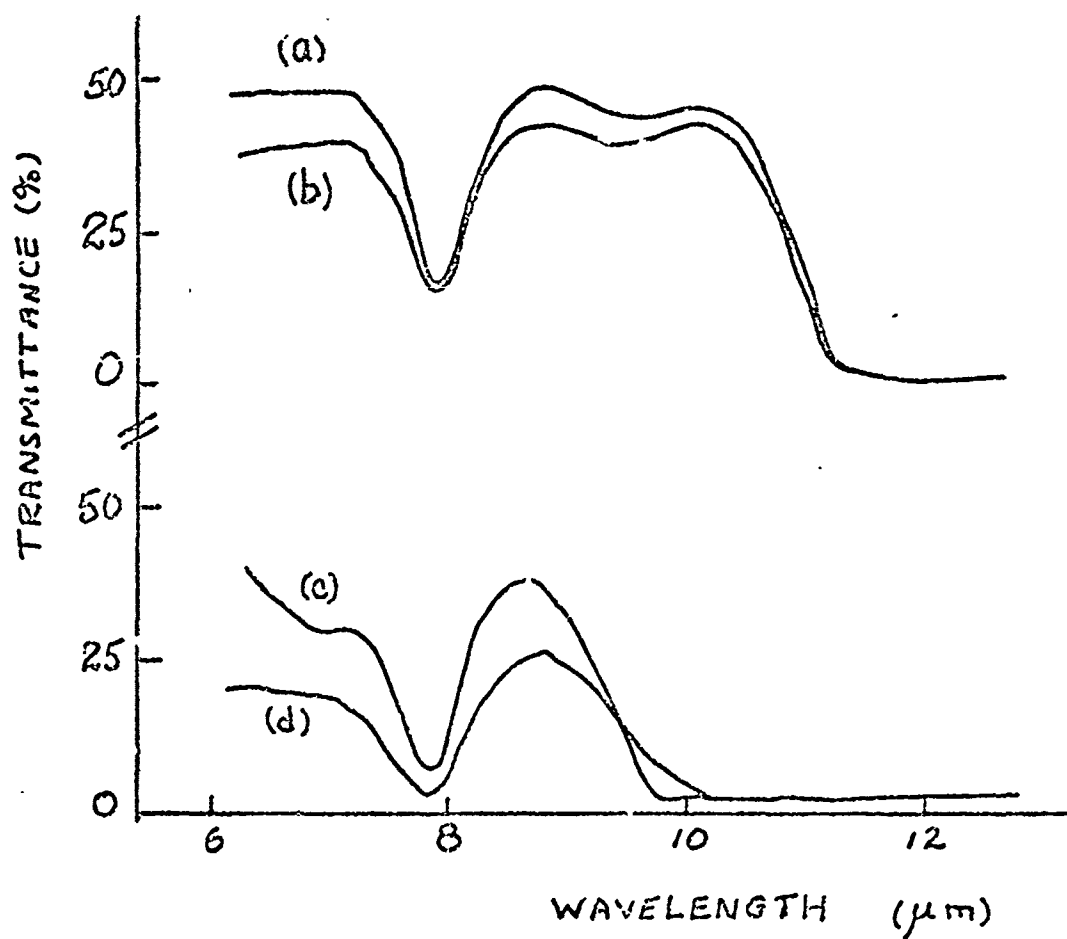


Figure 8. Infrared Transmittance of Ge-Se-As Glasses. Curve b - $\text{Ge}_2\text{Se}_3\text{As}$ as cast. Curve a - $\text{Ge}_2\text{Se}_3\text{As}$ after polishing. Curve d - $\text{Ge}_{33}\text{Se}_{55}\text{As}_{12}$ as cast. Curve c - $\text{Ge}_{33}\text{Se}_{55}\text{As}_{12}$ after 9 hours heat treatment at 400°C

Appendix B

Minimization of Reflectance Losses with Multilayer Coatings

The reflectance R of a semi-infinite substrate (potential window material) coated with two dielectric layers (see Figure B-1) is given by*

$$R = \frac{A}{B} \quad (1)$$

$$\text{where } A = r_1^2 + r_2^2 + r_3^2 + (r_1 r_2 r_3)^2 + 2r_1 r_2 (1 + r_3^2) \cos 2\phi + 2r_2 r_3 (1 + r_1^2) \cos 2\psi + 2r_1 r_3 \cos 2(\phi + \psi) + 2r_1 r_2^2 r_3 \cos 2(\phi - \psi)$$

$$B = 1 + (r_1 r_2)^2 + (r_1 r_3)^2 + (r_2 r_3)^2 + 2r_1 r_2 (1 + r_3^2) \cos 2\phi + 2r_2 r_3 (1 + r_1^2) \cos 2\psi + 2r_1 r_3 \cos 2(\phi + \psi) + 2r_1 r_2^2 r_3 \cos 2(\phi - \psi)$$

and

$$r_1 = \frac{n_0 - n_1}{n_0 + n_1}; \quad r_2 = \frac{n_1 - n_2}{n_1 + n_2}; \quad r_3 = \frac{n_2 - N}{n_2 + N}$$

$$\phi = \frac{2\pi n_1 d_1}{\lambda}; \quad \psi = \frac{2\pi n_2 d_2}{\lambda}$$

and

n_0 = refractive index of atmosphere (taken to be unity)

n_1 = refractive index of outer film

n_2 = refractive index of inner film (film nearest substrate)

N = refractive index of substrate

d_1 = thickness of outer film

d_2 = thickness of inner film

λ = wavelength of incident radiation.

*J. T. Cox, G. Hass and R. F. Rowntree, Vacuum, 4, 446 (1954).

If both films have an optical thickness of $\lambda/4$ -wavelength, i.e., if $n_1 d_1 = \lambda/4$, then equation (1) reduces to

$$R = \left[\frac{n_1^2 N - n_2^2}{n_1^2 N + n_2^2} \right]^2 \quad (2)$$

In this case, R will become zero if $n_2 = n_1 \sqrt{N}$.

By setting n_1 equal to unity in equation (2), one obtains the case of a substrate of refractive index N coated with a single film of refractive index n_2 and optical thickness $\lambda/4$. In this case, R becomes zero only in $n_2 = \sqrt{N}$. If, for example, the substrate is KCl ($N = 1.49$), n_2 must be 1.22 in order to have zero R . Since such a small refractive index is less than the refractive index of any solid film one could apply, it is evident that no single dielectric film deposited on an alkali halide substrate will reduce the reflectance to zero.

It is possible to obtain zero reflectance in the case of a double-layer coating even if $n_2 \neq n_1 \sqrt{N}$, if one film has an optical thickness greater than $\lambda/4$ and the other film has an optical thickness less than $\lambda/4$. A computer program has been written which, given a particular set of refractive indices (n_1, n_2, N), will determine the value(s) of (d_1, d_2) which minimize R using equation (1). A second program has been written which determines the sensitivity of R to deviations of d_1 and d_2 from those values which minimize R . This program also tells how R varies with λ , given a particular (n_1, n_2, N) and (d_1, d_2).

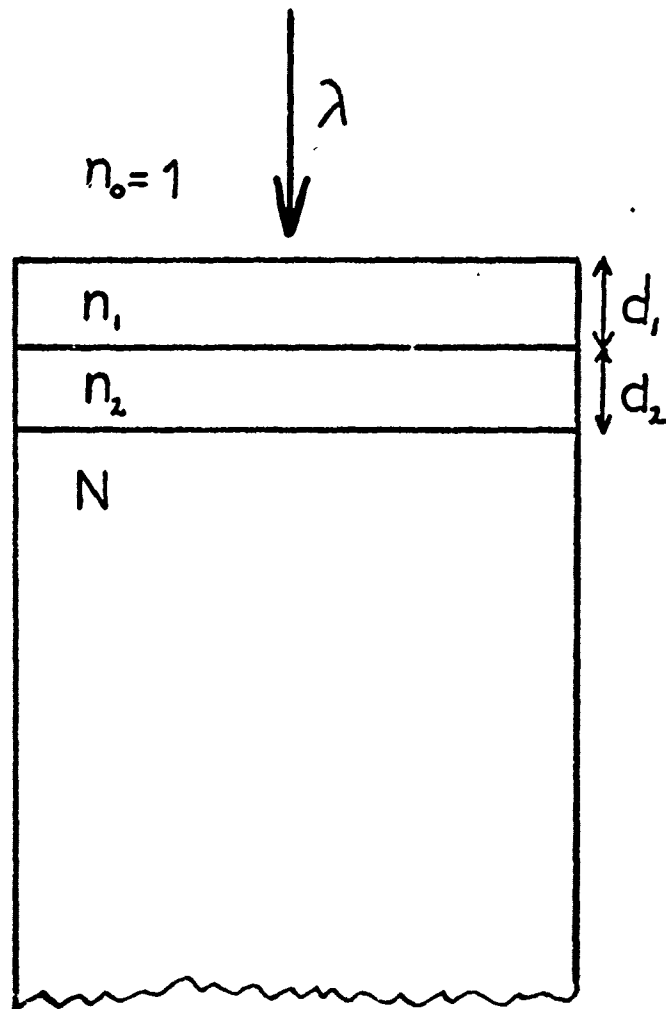


Fig. B-1. Two-layer antireflection coating on a semi-infinite substrate (symbols defined in text).

Unclassified

Security Classification

DOCUMENT CONTROL DATA - R & D		
<i>(Security classification of title, body of abstract and indexing annotation must be entered when the overall report is classified)</i>		
1. ORIGINATING ACTIVITY (Corporate author) Engineering and Industrial Experiment Station, University of Florida Gainesville, Florida 32601		2a. REPORT SECURITY CLASSIFICATION unclassified
		2b. GROUP
3. REPORT TITLE EVALUATION OF LASER WINDOW MATERIALS		
4. DESCRIPTIVE NOTES (Type of report and inclusive dates) Scientific. Final. 1 July 1971 - 30 June 1972 - Approved 24 Oct. 1972		
5. AUTHOR(S) (First name, middle initial, last name) Larry L. Hench Derek B. Dove Ronald E. Loehman		
6. REPORT DATE August 1, 1972	7a. TOTAL NO. OF PAGES 64	7b. NO. OF REFS 25
8a. CONTRACT OR GRANT NO F19628-71-C-0256	9a. ORIGINATOR'S REPORT NUMBER(S)	
b. PROJECT NO. 3326-05-01		
c. DOD ELEMENT 62601F	9b. OTHER REPORT NO(S) (Any other numbers that may be assigned this report) AFCRL-72-0452	
d.		
10. DISTRIBUTION STATEMENT Distribution limited to U.S. Government agencies only. Test and Evaluation: 19 September 1972. Other requests for this document must be referred to the Contract Monitor, AFCRL(LQP) L.G. Hanscom Field, Bedford, Massachusetts 01730		
11. SUPPLEMENTARY NOTES This research was supported by AFWL/AFCRL-71-8.		12. SPONSORING MILITARY ACTIVITY Air Force Cambridge Research Laboratories (LI) (LQ) L. G. Hanscom Field Bedford, Massachusetts 01730
13. ABSTRACT Chalcogenide glasses within the Ge-Se-As-Sb system have been prepared and characterized before and after heat treatment; they are homogeneous to a fine scale, but appreciable optical absorption at 10.6 μ m is present, due to oxygen impurities. The effect of gettering additions of Ti and Zr in the glasses to decrease the IR absorption has been examined. Heat treatment shows that the glasses are stable against devitrification and may withstand many hours of thermal exposure at 300°C without significant change in mechanical properties. A novel attempt to increase the toughness and water resistance of sintered alkali halide windows has been carried out by coating the alkali halide grains with polyethylene prior to hot pressing. Results, however, have been disappointing owing to the difficulty of obtaining a really coherent coating. The results of limited tests of the increase in water resistance imparted by coatings of deposited chalcogenide glasses are reported.		

KEY WORDS

Laser Window Materials

Chalcogenide Glasses

Thermal Stability

Alkali Halide Intergranular
CoatingsThermal Influence on Mechanical
Properties

LINK A

ROLE

WT

LINK B

ROLE

WT

LINK C

ROLE

WT